

Copyright
by
Rachel Elizabeth Hure
2017

**The Thesis Committee for Rachel Elizabeth Hure
Certifies that this is the approved version of the following thesis:**

Beyond the PG Specification for Asphalt Binders

**APPROVED BY
SUPERVISING COMMITTEE:**

Supervisor:

Amit Bhasin

Andre Smit

Beyond the PG Specification for Asphalt Binders

by

Rachel Elizabeth Hure, B.S.

Thesis

Presented to the Faculty of the Graduate School of

The University of Texas at Austin

in Partial Fulfillment

of the Requirements

for the Degree of

Master of Science in Engineering

The University of Texas at Austin

May 2017

Dedication

I would like to dedicate it to my family.

Acknowledgements

I would first like to thank Dr. Amit Bhasin for believing in me from the beginning. He never once questioned my abilities and potential. He has invested so much energy to ensure that I succeed and I will always be grateful.

I would like to acknowledge the Texas Department of Transportation (TxDOT) for partially supporting this study.

I would also like to acknowledge the Southern Plains Transportation Center (SPTC) for partial financial support.

In addition, I would like to thank my fellow lab mates Roy Rodriguez, Nazmus Sakib, Ramez Hajj, Sal Tijerina, Angelo Filonzi, and SangKi Lee for assisting me along the way. Their opinion and expertise are always appreciated. Further, I would like to thank undergraduate students Samantha Morey and Peter Hartley who helped out during this study.

I am grateful to my reader Dr. Andre Smit for his helpful edits and comments. Additionally, I would like to thank Phil Tomlin for his invaluable help around the lab with various challenges.

Also, I extend my appreciation to my friends and family for supporting me throughout the research process and always pushing me to be my best. Lastly, I would like to thank my fiancé Andrew Cook for his huge amount of patience and graciousness throughout my higher education pursuit.

Abstract

Beyond the PG Specification for Asphalt Binders

Rachel Elizabeth Hure, M.S.E.

The University of Texas at Austin, 2017

Supervisor: Amit Bhasin

Classification of asphalt binder has evolved since the invention of asphalt pavement in 1870. Starting with penetration grading, moving forward to viscosity grading, and now the current system of performance grading (PG). All states in the US now adhere to some form of the PG system. During the last decade, several new modifiers and extenders have been introduced to modify the grade of a straight-run binder to achieve a target PG. In some cases, it has been observed that although a binder may meet the current PG specification, it may result in significantly sub-par performance. This suggests that the current PG specification does not accurately capture the performance characteristics of a binder. The main objective of this study was to use alternative chemical and mechanical tests on a large set of binders to identify differences in binders with a similar PG. This study examined the performance of 34 asphalt binders from 12 different binder sources using standard PG tests following AASHTO M320, as well as tests beyond the PG specification. The tests outside of the PG framework included chemical tests (X-ray fluorescence and spot), as well as other mechanical tests (Multiple Stress and Creep Recovery to measure permanent deformation potential at multiple high temperatures, BBR Pro to measure tensile strength

at low temperatures, and poker chip test to measure tensile strength at intermediate temperature). For tests outside the PG specification, outlier criteria were developed based on the results found. Outliers were defined differently for each test and do not represent positive or negative outcomes in terms of expected performance. The tests outside of the PG specification (spot, ΔT_c , aging sensitivity, poker chip, and low temperature strength) all produced many outliers, some even extreme outliers for binders with a similar PG. This study highlights the need for additional testing beyond the PG specification to improve binder grading. More performance testing on mixtures is needed to establish if outlier behavior is beneficial or detrimental.

TABLE OF CONTENTS

List of Figures	x
List of Tables	xiv
Chapter 1. Introduction and Literature Review	1
1.1 Background on Performance Grading of Asphalt Binders	1
1.2 Developments Since Introduction of the Performance Grade System	5
1.2.1 Rutting Characteristics	6
1.2.2 Cracking Characteristics	8
1.2.3 Low Temperature Characteristics	11
1.2.4 Summary of Performance Characteristics in the PG System	13
1.3 Motivation	13
Chapter 2. Materials, Methods and Parameters	15
2.1 Materials	15
2.2 PG Tests	15
2.3 Additional Tests and Parameters Beyond PG Specifications	20
2.3.1 Metal Content	20
2.3.2 MSCR-Based True Grade	22
2.3.3 Spot Test	24
2.3.4 ΔT_c	25
2.3.5 Aging Sensitivity	26
2.3.6 Strength Test at Intermediate Temperature	27
2.3.7 Strength Test at Low Temperature	27
Chapter 3. Laboratory Testing Results	30
3.1 Overview	30
3.2 Laboratory Testing Results	30
3.2.1 Metal Content	30
3.2.2 MSCR-Based True Grade	34
3.2.3 Spot Test	38
3.2.4 ΔT_c	41

3.2.5	Aging Sensitivity	44
3.2.6	Strength Test at Intermediate Temperature	47
3.2.7	Strength Test at Low Temperature	50
3.2.7.1	PAVI	50
3.2.7.2	PAVII	54
Chapter 4.	Conclusions and Summary	58
4.1	Overview	58
References		61

LIST OF FIGURES

Figure 1.1.	Each states grading system in 1985 (Brown et al., 2009).	3
Figure 2.1.	The PG grades of all the binders used in the study.	16
Figure 2.2.	The James Cox & Sons Rolling Thin Film Oven, Model CS 325. . .	16
Figure 2.3.	The Prestex Pressure Aging Vessel by the Gilson Company.	17
Figure 2.4.	The AR 2000 Dynamic Shear Rheometer.	17
Figure 2.5.	A log-linear plot of $\frac{G^*}{\sin \delta}$ versus temperature for RTFO-aged binder E 64-22.	18
Figure 2.6.	The CANNON Instrument Company Bending Beam Rheometer (BBR), Model TE.	19
Figure 2.7.	A log-linear plot of stiffness versus temperature for binder D 76-22.	19
Figure 2.8.	A linear plot of m-value versus temperature for binder D 76-22. . .	20
Figure 2.9.	The Brunker X-ray fluorescence spectrometer.	21
Figure 2.10.	The percent strain over time of binder J 70-22 for the first cycle. .	23
Figure 2.11.	A log plot of J_{nr} versus temperature for binder J 70-22.	24
Figure 2.12.	The dissolved binder beside the marked filter paper.	25
Figure 2.13.	Spots at various steps of the process from scan to grayscale to ImageJ.	25
Figure 2.14.	The different degrees of separation from homogeneous to separated.	25
Figure 2.15.	The Instron E1000 set up (Sultana, 2014).	28
Figure 2.16.	A schematic of the plate geometry (Sultana, 2014).	28
Figure 2.17.	The CANNON Instrument Company Bending Beam Rheometer (BBR) Pro, model TE.	29
Figure 3.1.	The XRF spectra for binders with a high temperature grade of PG 58.	31
Figure 3.2.	The XRF spectra for the first half of binders with a high tempera- ture grade of PG 64.	31
Figure 3.3.	The XRF spectra for the second half of binders with a high tem- perature grade of PG 64.	31
Figure 3.4.	The XRF spectra for first half of binders with a high temperature grade of PG 70.	32

Figure 3.5.	The XRF spectra for second half of binders with a high temperature grade of PG 70.	32
Figure 3.6.	The XRF spectra for binders with a high temperature grade of PG 76.	32
Figure 3.7.	A summary of all the binders tested and the metals found through the XRF test.	33
Figure 3.8.	The true grades for all high temperature PG 58 binders.	35
Figure 3.9.	The true grades for all high temperature PG 64 binders.	36
Figure 3.10.	The true grades for all high temperature PG 70 binders.	36
Figure 3.11.	The true grades for all high temperature PG 76 binders.	37
Figure 3.12.	A summary of all the binders tested and outliers present for high temperature PG grading.	37
Figure 3.13.	The percent black area for all high temperature PG 58 and PG 64 binders.	39
Figure 3.14.	The percent black area for all high temperature PG 70 and PG 76 binders.	39
Figure 3.15.	The results for percent black area of the total area with outliers in red.	40
Figure 3.16.	The difference in m-value and stiffness true grades for PG 64-22 binders.	42
Figure 3.17.	The difference in m-value and stiffness true grades for the remaining low temperature PG -22 binders.	42
Figure 3.18.	The difference in m-value and stiffness true grades for low temperature PG -28 grade.	43
Figure 3.19.	A summary of all the results for ΔT_c with outliers in red.	43
Figure 3.20.	The change in m-value and stiffness between aging conditions for PG 64-22 binders.	44
Figure 3.21.	The change in m-value and stiffness between aging conditions for the remaining low temperature PG -22 grade binders.	45
Figure 3.22.	The change in m-value and stiffness between aging conditions for low temperature PG -28 grade binders.	45
Figure 3.23.	A summary of results for changes in low temperature properties with outliers in red and brown.	46
Figure 3.24.	The tensile strength at fracture for PG 58-28 binders.	47

Figure 3.25.	The tensile strength at fracture for PG 64-22 binders.	48
Figure 3.26.	The tensile strength at fracture for PG 70-22 binders.	48
Figure 3.27.	The tensile strength at fracture for PG 76-22 binders.	49
Figure 3.28.	A summary of the poker chip test results with outliers in red. . . .	49
Figure 3.29.	The maximum stress at fracture for PG 64-22 PAVI-aged binders tested at -12°C (10°C above the label temperature).	50
Figure 3.30.	The maximum stress at fracture for the remaining low temperature PG -22 PAVI-aged binders tested at -12°C (10°C above the label temperature).	51
Figure 3.31.	The maximum stress at fracture for low temperature PG -28 PAVI- aged binders tested at -18°C (10°C above the label temperature). .	51
Figure 3.32.	The maximum stress at fracture for PG 64-22 PAVI-aged binders tested at -18°C (4°C above the label temperature).	52
Figure 3.33.	The maximum stress at fracture for the remaining low temperature PG -22 PAVI-aged binders tested at -18°C (4°C above the label temperature).	52
Figure 3.34.	The maximum stress at fracture for low temperature PG -28 PAVI- aged binders tested at -24°C (4°C above the label temperature). . .	53
Figure 3.35.	Summary of all the strength testing on PAVI-aged binder in the BBR Pro at -12, -18, and -24°C.	53
Figure 3.36.	The maximum stress at fracture for PG 64-22 PAVII-aged binders tested at -12°C (10°C above the label temperature).	54
Figure 3.37.	The maximum stress at fracture for the remaining low temperature PG -22 PAVII-aged binders tested at -12°C (10°C above the label temperature).	55
Figure 3.38.	The maximum stress at fracture for low temperature PG -28 PAVII- aged binders tested at -18°C (10°C above the label temperature). .	55
Figure 3.39.	The maximum stress at fracture for PG 64-22 PAVII-aged binders tested at -18°C (4°C above the label temperature).	56
Figure 3.40.	The maximum stress at fracture for the remaining low temperature PG -22 PAVII-aged binders tested at -18°C (4°C above the label temperature).	56
Figure 3.41.	The maximum stress at fracture for low temperature PG -28 PAVII- aged binders tested at -24°C (4°C above the label temperature). . .	57

Figure 3.42. Summary of all the strength testing on PAVII-aged binders in the
BBR Pro at -12, -18, and -24°C. 57

LIST OF TABLES

Table 2.1.	All the metals in each asphalt modifier (Arnold and Shastry, 2015).	21
Table 3.1.	The metals detected and the corresponding modifier.	34
Table 4.1.	A summary of the outliers for all the tests run in this study.	60

CHAPTER 1. INTRODUCTION AND LITERATURE REVIEW

1.1 BACKGROUND ON PERFORMANCE GRADING OF ASPHALT BINDERS

Pennsylvania Avenue, Washington D.C. saw the first Hot Mix Asphalt (HMA) pavement back in the 1870s. The mix used naturally occurring asphalt from the lake on the Island of Trinidad. When demand exceeded supply for lake asphalts in the late 1800s, petroleum products came onto the asphalt scene (Blow, 2016). By 1888, H.C. Bowen invented the Bowen Penetration Machine. It was used to test the consistency of asphalt cement. Prior to Bowen's Penetration Machine, asphalt quality was tested using the chewing method. Asphalt road constructors actually bit into the binder (Brown et al., 2009). American Society for Testing Materials (ASTM) adopted the penetration test in 1903 (Blow, 2016). In 1910, the penetrometer was released, a more refined version of the Bowen Penetration Machine. It tested the penetration of asphalt binders at 25°C. By 1918, the Bureau of Public Roads, now known as the Federal Highway Administration (FHWA), introduced the penetration grade system based on the climatic conditions of the region. American Association of State Highway Officials (AASHO), now known as American Association of State Highway and Transportation Officials (AASHTO), followed suit in 1931 by publishing a standard (Blow, 2016). The latest standard method is ASTM D5. There are five penetration grades which depend on the penetration test results. ASTM D946 lays out the current specifications followed in the United States. Other tests are also run to check conformance in terms of the softening point, flash point, and solubility.

The benefit of the penetration grading system is that the consistency of the asphalt binder is measured at the average service temperature. Also, the testing time is short and low cost. In addition, the penetration system is adaptable to field applications. Unfortunately, there are also many disadvantages. The shear rate is high and very variable. Additionally, penetration at 25°C shows deceptive performance at higher and lower service temperatures. Lastly, the test is empirical and fails to measure the asphalt consistency at the maximum temperature, which occurs during mixing and compaction of asphalt mixtures (Brown et al., 2009).

In order to address the void in asphalt binder properties at the maximum temperature, the viscosity grading system was developed in the 1960s. The goal was to replace the empirical penetration test with a rational scientific viscosity test. In this way, the asphalt binder consistency at 60°C could be measured, better protecting against rutting. The

viscosity grading system was the most popular in the United States prior to the current performance-based system (also known as AC grading). ASTM D3381 details the specifications based on the viscosity at 60°C. Other tests are conducted as checks with minimum requirements such as the viscosity at 135°C, penetration at 25°C, flash point, and solubility. Penetration at 25°C is important because it controls the asphalt consistency near the service temperature, whereas the viscosity at 135°C controls the asphalt consistency near the mixing and compacting temperatures (Brown et al., 2009).

The benefit of the viscosity grading system is that it measures a fundamental property of the material, not empirical parameters. The results are independent of the test system and sample size. Also, the system works for a wide range of environments with pavement temperatures from 25°C to 60°C. In addition, a wide range of test instruments may be used. Furthermore, asphalt binder consistency is measured at three different temperatures so the temperature susceptibility can be determined. Lastly, the risk for rutting is reduced compared to the penetration grading system since viscosity is measured at the maximum pavement temperature experienced during service. But with any system there are always trade-offs. First, the testing time is longer and more costly than with the penetration grade system. Second, grading at 60°C does not represent the performance at average or lower service temperatures, which would be at or below 25°C. Thus, the system fails to prevent low temperature cracking since testing is not done at low temperatures (Brown et al., 2009).

The California Department of Highways (now Caltrans) worked with the Pacific Coast User Producer Group to develop a similar viscosity grading system in the same time frame as the other viscosity grading system (AC), except this system focused on aged asphalt binder. The Aged Residue (AR) viscosity grading system was motivated by mix setting problems Caltrans was experiencing, where the viscosity was not increasing uniformly between asphalt binders during the mixing process. By performing grading after the binder had undergone short-term aging using the Rolling Thin Film Oven (RTFO), the aim was to replicate the same behavior as during construction in the field. The current standard followed in the United States is ASTM D3381, where the viscosity test is performed on aged residue at 60°C. Like the standard viscosity grading system, a penetration test at 25°C and viscosity test at 135°C are also completed to ensure the minimum values are met for the specified grade. The only difference is all the tests are done on aged asphalt binder; no consistency values are gathered for original asphalt binder (Brown et al., 2009).

Some of the advantages of the AR viscosity grading system are that the asphalt properties seen after HMA is manufactured are well represented by the aged residue prop-

erties in the lab. Also, reasonable uniform behavior is expected between asphalt from different sources that fall within the same AR viscosity grade. On the down side, the grading system is highly regional and requires more equipment than the penetration or viscosity grading systems since an aging device must be used. Third, the testing time is the longest out of the three systems mentioned so far since all the asphalt binder must undergo aging before any tests can be run. Fourth, because there are no tests run on original asphalt binder, detecting contamination is near impossible (Brown et al., 2009).

Even with all the advances in the grading systems, better characterization of asphalt binders still continued to improve in hopes of reaching a more universal system that fit all climatic conditions. Each state and/or region had differing specifications to accommodate the area's conditions. By 1985, states followed either one of the three systems (penetration, AC, AR) or a combination of the three as seen in Figure 1.1.

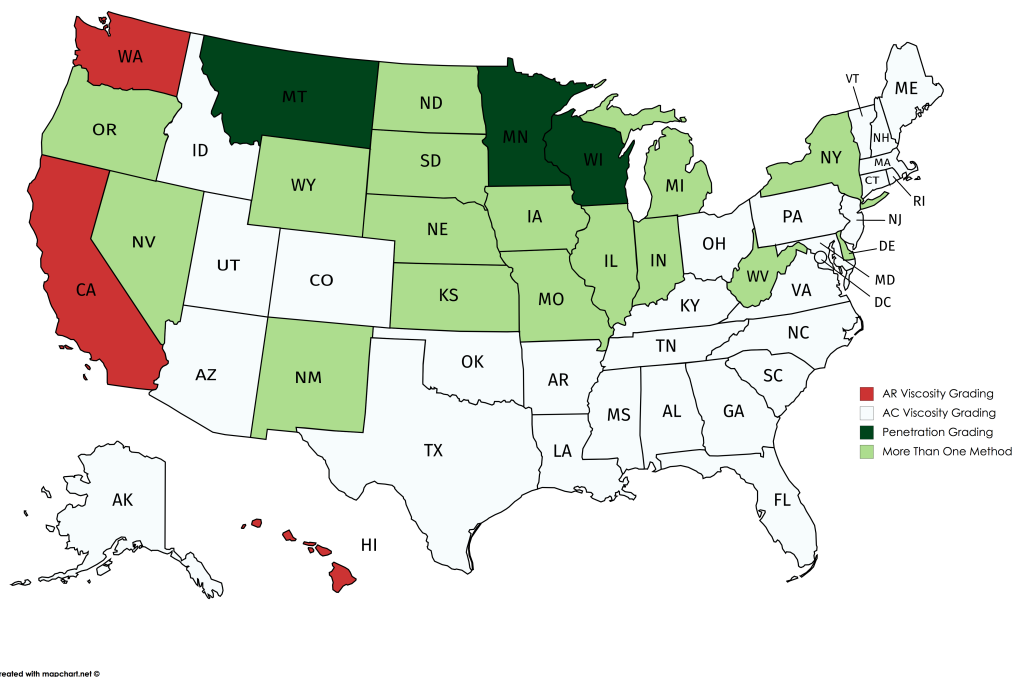


Figure 1.1. Each states grading system in 1985 (Brown et al., 2009).

Federal leaders saw a need for a more robust system that could accommodate many diverse climates and asphalt binder sources. The Superpave specification is a product of the Strategic Highway Research Program (SHRP) Asphalt Research program. The program was launched in 1987 with a budget of \$50 million over a 5-year period. By the mid-

1990s, the PG grading system was released (Brown et al., 2009). The goal of the new methods was to improve performance, be applicable to any area (taking into account traffic, environment, and the structural section), and replace the various material specifications and mixture design methods utilized across the United States. The performance grading (PG) system is meant to represent a universal system for any region while still improving performance. Currently, all states in the US have adopted a version of the PG system. Nonetheless, many countries worldwide have not yet adopted the Superpave methods.

The three main test devices in the PG system are the Bending Beam Rheometer (BBR), Dynamic Shear Rheometer (DSR), and Direct Tension test (DTT). These devices are used to measure fundamental material properties, which are then used in a performance-based specification framework. This allows any asphalt binder to be compared objectively to other binders, whether they are unmodified or modified. The BBR test measures the creep stiffness and m-value (slope of the stiffness versus temperature log-log plot) to prevent low-temperature cracking. The DSR test quantifies the shear stiffness and phase angle to calculate $\frac{G^*}{\sin \delta}$ and $G^* \sin \delta$ to screen for susceptibility to permanent deformation and fatigue cracking. Lastly, the DTT measures failure strain to avoid low-temperature cracking (Kennedy et al., 1994). AASHTO M320 designates the PG grade based on specified criteria for each of the tests (BBR, DSR, DTT).

Following AASHTO M320, the BBR specification limits the stiffness of an asphalt binder beam to a maximum of 300 MPa and the m-value to a minimum of 0.3 at the specified low temperature. Asphalt binder undergoes long-term aging using the Pressure Aging Vessel (PAV) before being tested in the BBR. The more conservative true grade produced from these two parameters determines the asphalt binder's PG low temperature grade. Then, the true grade is rounded up to an increment of 6°C (ASTM 7643, 2010).

The AASHTO standard specifies DSR limits of $\frac{G^*}{\sin \delta}$ to a minimum of 2.2 kPa at a specified high temperature. Original and short-term aged binder (using the RTFO) are tested in the DSR. Similar to the BBR test, the true grade is rounded by an increment of 6°C, but rounded down to stay on the conservative side. As a fatigue cracking check, $G^* \sin \delta$ must be less than the maximum of 5,000 kPa at the specified intermediate temperature.

Finally, the DTT must produce a minimum tensile strain of 1 percent at failure. The DTT results are compared against the BBR measured properties, but DTT is not necessary if the stiffness of the binder is less than 300 MPa at the minimum pavement design temperature (Kennedy et al., 1994). The high grade determined from the DSR test and the low grade from the BBR test come together for the complete PG grade. Carried over from the

viscosity grading system, the viscosity is still measured at 135°C as a check in place to ensure a maximum of 3 Pa-s is not exceeded.

The benefit of the PG grading system lies in its universality. Previous systems performed each test at just one temperature, but the PG system conducts each test at various temperatures to account for different climates. Also, by splitting the grading into two numbers, both high and low temperature properties are considered during the grading process, hopefully preventing rutting and low temperature cracking. All the previous systems tested at the maximum and average service temperatures, but not low temperatures. In addition, all phases of the aging process are tested from the original binder to short-term aged (RTFO) to long-term aged (PAV). In this way, from the time the asphalt binder is added to the mix to field compaction to twenty years into the service life, testing is done to correlate performance (Brown et al., 2009). The grading system has seen many steps forward with the PG grading system, but improvements can always be made.

1.2 DEVELOPMENTS SINCE INTRODUCTION OF THE PERFORMANCE GRADE SYSTEM

As mentioned, the PG grading system was a huge leap forward from the penetration and AR and AC viscosity grading systems. In the PG grading system, fundamental properties of asphalt binder are tested at multiple temperatures and aging conditions to characterize both low and high temperature properties. Testing became more involved and expensive with the transition from penetration and/or viscosity grading to PG grading. But every system has opportunities for improvement. Starting with the high temperature side of the PG grading system, $\frac{G^*}{\sin \delta}$ is currently calculated by measuring G^* and δ in the DSR according to AASHTO M320. Bahia et al. (2001) found that $\frac{G^*}{\sin \delta}$ and rutting had a weak correlation, so another test was developed to improve the indicator for resistance to permanent deformation called the Multiple Stress Creep and Recovery (MSCR). The $\frac{G^*}{\sin \delta}$ parameter is still used on original binders, but a different criterion is used for RTFO-aged binders through the MSCR test.

Moving onto the intermediate temperature component of the PG grading system, fatigue cracking is the largest concern. The current specification measures G^* and δ to calculate $G^* \sin \delta$. The Superpave method works well to characterize unmodified binders, but not chemical or polymer modified binders. The $G^* \sin \delta$ parameter assumes that dissipated energy is due to incremental damage and the recoverable viscoelastic dissipation is small. Other methods have been developed to overcome these challenges as modified

binders become more prevalent (Hajj and Bhasin, 2017).

Looking at the low temperature side of the PG grading system, stiffness is used to characterize binder performance. According to the Superpave system, the binder performance is dependent on the stiffness and m-value (Kennedy et al., 1994). Yet, the strength of asphalt pavement determines when low-temperature cracking occurs, not the stiffness. Strength of asphalt binders is rarely measured, resulting in inconsistencies between lab and field performance. The asphalt binder specifications need to factor in strength, not stiffness of asphalt binders (this is true for high, intermediate, and low temperature properties).

Along with the BBR, the Direct Tensile Test (DTT) is used for determining low temperature properties of asphalt binders. As mentioned before, the DTT is not needed if the stiffness of the binder is less than 300 MPa at the minimum pavement design temperature (Kennedy et al., 1994). The resulting failure strain of the DTT is used to determine binder properties with no consideration of strength. Strength is merely an input in the NCHRP Mechanistic Empirical Pavement Design Guide (Falchetto et al., 2014). Normally, the fracture properties of binders are not considered since BBR alone can characterize the low-temperature properties (only taking into account rheological properties).

More issues arise with the current Superpave system. For the BBR test, only one parameter ends up determining the asphalt binder's low temperature PG grade. Normally, the m-value determines the true grade. Marasteanu (2004) claims that thermal stresses are controlled more by stiffness than m-value, since a lower stiffness produced a lower thermal stress. Contrary to popular belief, when comparing the binders with similar stiffness values, Marasteanu (2004) found that a lower m-value resulted in lower thermal stress due to a slower accumulation of stresses. Regardless, stiffness and m-value may not be the best predictors of low-temperature cracking since strength needs consideration and m-value proves to be inaccurate in predicting the low-temperature PG grade. The following sections discuss these issues in more detail.

1.2.1 Rutting Characteristics

The high temperature portion of the PG grading is meant to prevent rutting since rutting occurs at high temperatures. As mentioned, AASHTO M320 is followed as part of the Superpave design to determine the high temperature grade based on both original and RTFO-aged binder testing through measurement of G^* and δ in order to calculate $\frac{G^*}{\sin \delta}$. This system worked well until the introduction of modified binders. In order to meet the required PG grade, chemical or polymer modifiers are now typically added to asphalt

binders. The Superpave design has limited applicability to most modified binders, since they have shown highly nonlinear and stress sensitive behavior to loading. In addition, variability in modified binder sensitivity has been exhibited due to traffic speed, traffic volume, and stress or strain level according to pavement structure (Bahia et al., 2001). Thus, as more asphalt producers add modifiers, another test has been developed to improve high temperature characterization. This is particularly important because not all modifiers are the same and while they may be used to design binders with a similar performance grade, the actual performance can vary significantly depending on the modifier.

The Multiple Stress Creep and Recovery (MSCR) test also utilizes the DSR, but measures different properties of the asphalt binder. MSCR measures the non-recoverable compliance, synonymous to elastic recovery, referred to as J_{nr} . J_{nr} is the non-recoverable strain at the end of a 9-second recovery period, followed by a 1-second loading period. The term non-recoverable compliance often times is used more strictly than in this case since recovery continues beyond the 9-second recovery period. But in the broadest sense, non-recoverable compliance is an equivalent term. The higher the J_{nr} , the more permanent deformation, and thus higher susceptibility to rutting (Arega et al., 2016).

One of the benefits of the MSCR test is the resulting elastic recovery and stress sensitivity. This avoids the need for a ductilometer to measure elastic recovery and the stress sensitivity measurement addresses modified binder concerns. In addition, grade bumping is not necessary (Arega et al., 2016). For the standard $\frac{G^*}{\sin \delta}$ PG test, traffic and loading may be accounted for through the practice of grade bumping. This is where the binder grade is "bumped" up one grade (i.e. PG 64 to PG 70) due to slow moving traffic since the rutting potential is high and two grades (i.e. PG 64 to PG 76) due to standing traffic since the rutting potential is even higher. But grade bumping has no effect on the low temperature PG grade since rutting is only of concern at high temperatures (Texas Department of Transportation, 2006).

For the MSCR test, instead of grade bumping, different criterion exist depending on the traffic condition. There are four traffic categories: S for standard, H for heavy, V for very heavy, and E for extreme (Arega et al., 2016). Nonetheless, the intended replacement of AASHTO M320, AASHTO MP19, still measures $\frac{G^*}{\sin \delta}$ on the original binder. AASHTO MP19 is a modified version of AASHTO M320 to incorporate the MSCR test into the specification. Unlike in AASHTO M320, where $\frac{G^*}{\sin \delta}$ is measured on RTFO-aged binder as well, for AASHTO MP19 MSCR is conducted on RTFO-aged binder. In this way, MSCR determines the RTFO-aged binder true grade and $\frac{G^*}{\sin \delta}$ determines the original binder true

grade. The lower of the two temperatures determines the high temperature grade as with the current specification AASHTO M320.

Studies by Zhou et al. (2014), Bukowski et al. (2011), D'Angelo (2010), and Dubois et al. (2014) confirm that the MSCR test has been found to better predict resistance to permanent deformation based on the J_{nr} values. AASHTO MP19 brings in the MSCR test, while still incorporating the $\frac{G^*}{\sin \delta}$ test. Stress sensitivity and nonlinear behavior of modified binders is addressed with the MSCR test.

1.2.2 Cracking Characteristics

Fatigue cracking is the most common form of failure for asphalt pavement. $G^* \sin \delta$ is used to indicate fatigue cracking resistance at intermediate temperatures by utilizing the DSR. Testing is done on asphalt binders because binders experience higher localized stress than the asphalt mixture as a whole (Bahia et al., 1999; Masad et al., 2001). Binder is the glue for the mixture and must hold together all of the aggregates. A cyclic load is applied to PAV-aged binder at 10 rad/s. The testing temperature is determined by the high and low temperature grades from PG grading (Equation 1.1).

$$T_i = \frac{\text{High Grade} - \text{Low Grade}}{2} + 4 \quad (1.1)$$

Although in some states, such as Texas, where high grades specified for construction often exceed PG 64 due to grade bumping to account for traffic loading, the intermediate testing temperature is based on a high temperature of 64°C and not the actual high grade of the binder (Texas Department of Transportation, 2014). Regardless of the temperatures tested at, AASHTO M320 specifies a maximum $G^* \sin \delta$ of 5,000 kPa. A maximum value is specified since higher $G^* \sin \delta$ is interpreted as an indicator of higher incremental damage and thus, the higher the incremental damage, the higher the susceptibility to fatigue damage. G^* is the magnitude of complex shear modulus, measuring the stiffness at a given loading frequency and temperature-aging condition. δ is the phase angle of the material at the same frequency that G^* is measured, calculated by the lag between the stress and strain (Hajj and Bhasin, 2017). These two properties of the asphalt binder are the same as those measured for calculating the high temperature grade, except that the values are multiplied, not divided. In addition, a smaller parallel plate is used for testing in the DSR since stiffer PAV-aged binder is used instead of RTFO-aged binder.

As mentioned earlier, $G^* \sin \delta$ is used to compare dissipated energy of different as-

phalt binders. For elastic materials, energy dissipated is a measure of the energy released due to incremental damage propagation. But asphalt binder is a viscoelastic material so energy dissipated must be assumed to be a result of incremental damage and little recoverable viscoelastic dissipation. These assumptions hold mostly true for unmodified binders, but not modified binders (Hajj and Bhasin, 2017). AASHTO M320 was designed without the knowledge of modified binders so it makes sense the specification needs some modification to meet the current characteristics of asphalt binders.

Researchers have investigated how well $G^* \sin \delta$ indicates fatigue cracking resistance. Bahia et al. (1999) found that $G^* \sin \delta$ does not measure the non-linear response of asphalt binder under high strain amplitudes. The current intermediate test is run under a low strain amplitude of one percent. The test method needs high strain levels to better understand how the material behaves once in the non-linear range. Stuart and Mogawer (2002) contributed to the exploration of the specification. They found that both strain-controlled parameter $G^* \sin \delta$ and stress-controlled parameter $\frac{G^*}{\sin \delta}$ could not independently explain temperature effects on fatigue cracking. Strain-controlled tests were conducted at intermediate temperatures, while stress-controlled tests were run at high or intermediate temperatures.

Tsai and Monismith (2005) discovered a poor correlation between $G^* \sin \delta$ and laboratory mixture performance. They agreed with Bahia et al. (1999) that high strain amplitudes need to be used to evaluate asphalt binders. In addition, only a few cycles are run to measure G^* and δ even though pavements experience many loading cycles. Moreover, testing at one temperature and one rate of loading provides little insight into the behavior of the material. Lastly, $G^* \sin \delta$ does not indicate the strength of the material since G^* is a measure of the stiffness of the material. Nonetheless, Tsai and Monismith (2005) realized that the current specification cannot simply be thrown out until a suitable replacement has been developed.

Investigation to improve upon the current PG specification falls into four categories. The first category deals with applying a cyclic loading to induce failure at constant frequency and amplitude or conducting time sweeps as is traditionally done in the DSR. Newer time sweep methods proved to be an advancement in the current Superpave design since correlations were found between the metrics developed to predict fatigue failure and the mixture performance. But the test was rather slow so monotonically increasing shear stress and amplitude sweep tests were investigated to overcome this weakness, leading to the next category.

The second category is progressively increasing stress or strain amplitudes until failure, also known as amplitude sweep tests. Once again metrics were developed for fatigue resistance of asphalt binders, but this time using simplistic and mechanistic models such as the Viscoelastic Continuum Damage (VECD) model. The main benefit of the amplitude sweep test is its speed since it is faster than the time sweep test. Looking at these two categories, frequency sweep or time sweep as well as other similar tests such as the monotonically increasing stress test, all use a parallel plate geometry which can lead to damage induced by edge instability. This form of damage is significantly different from fatigue cracking. In addition, torsional shear and the specimen thickness pose challenges for these tests since edge failure and flow may occur. Thus, they may be a better indicator of damage resistance, not fatigue damage resistance (Hajj and Bhasin, 2017).

Moving onto the third category, this category groups all measurements of ductility of binder or surrogate ductility to indicate resistance to cracking. A correlation was found between ductility at low-intermediate temperatures (15°C) and cracking in asphalt pavement for both direct and indirect measurement. For direct measurement, essential and plastic works of fracture parameters were measured, showing a strong relation between laboratory mixture performance and field performance. A disadvantage of direct measurement of ductility is the large number of samples required and immense time needed. Indirect measurements of ductility can come in the form of rheological parameters such as $\frac{G'}{\eta'}$. Benefits of indirect measurement are the small number of samples needed and the utilization of the DSR, which is already used by the current PG system. $\frac{G'}{\eta'}$ has been shown to correlate well with unmodified binders, but investigation into the correlation with modified binders is still underway (Hajj and Bhasin, 2017).

The last category puts together methods of measuring strength or fatigue cracking resistance of asphalt binder in a realistic stress state. A realistic stress state refers to subjecting a thin film of mixture under a state of confinement to a stress similar to that experienced in the field. The goal is to recreate damage nucleation and propagation to determine the strength of the thin film of binder in a confined state. Some of the methods developed are double cantilever, butt joint, and poker chip. In addition, a standardized composite consisting of glass beads instead of aggregates is used to reach the same goal of recreating damage nucleation and propagation. The methods in this category show strong correlation with mixture fatigue performance and encourage accuracy, but require very different equipment and methods than currently employed by the PG grading system (Hajj and Bhasin,

2017).

Continuing to improve methods to better measure fatigue damage resistance is very important for many reasons. First, fatigue damage is used for grading, purchase, and design of asphalt binders. Also, it serves as a screening tool to evaluate the influence of modifiers and/or additives. Lastly, measuring fundamental material properties of asphalt binder are essential as model inputs for behavior and damage evolution in the mixture (Hajj and Bhasin, 2017).

1.2.3 Low Temperature Characteristics

When selecting the best asphalt binder for a particular use with low temperature properties in mind, mitigation of low-temperature cracking is the biggest concern. Breaking down the mechanics of low-temperature cracking, the change in temperature induces thermal stresses in a pavement. As a pavement cools down, the inability of the pavement to change its geometry causes thermal stresses to build up in the asphalt binder. Once the stresses exceed the strength of the binder, a crack is initiated (Anderson et al., 2011). But the natural ability of a binder to relax allows these thermal stresses to dissipate over time, preventing a build up of high stresses. Thus, a desirable pavement has superior relaxation and strength properties (Jones et al., 2014).

According to the current Superpave specifications, stiffness and m-value of asphalt binders are measured using the Bending Beam Rheometer (BBR) test to determine low-temperature stiffness properties (Kennedy et al., 1994). The BBR applies a point load to asphalt binder beams in a bath at low temperatures. A low stiffness represents lower induced stress and thus a favorable property since stress is essentially the product of the: change in temperature, coefficient of thermal expansion, and stiffness. A high m-value indicates a desirable property due to the elevated ability to relax, resisting the generation of stresses. Mathematically speaking, the m-value represents the slope of the stiffness versus loading time in the log-log plot, or the rate of relaxation (Kennedy et al., 1994).

Stiffness is used to characterize binder performance. As mentioned before, thermal stresses developed in the binder in the field depend on the stiffness and m-value for the PG system (Kennedy et al., 1994). However, failure or cracking only occurs when the thermal stresses exceed the capacity or tensile strength of the binder, which can be different from one binder to another. But strength of asphalt binders is often not measured, so correlation between laboratory and field performance is poor. Strength must be factored into the specification of asphalt binders. Also, normally only the m-value ends up determining the

asphalt binder's low temperature PG grade. Nonetheless, stiffness and m-value may not be the best predictors of low-temperature cracking since strength needs consideration and m-value proves to be inaccurate in predicting the low-temperature PG grade.

Other studies point to the use of ΔT_c as a better indicator of field performance. In the presentation made by Rowe (2016), ΔT_c is defined as the difference between the critical temperature based on the stiffness and the critical temperature based on the m-value as measured in the BBR test. As mentioned early, the more conservative value (warmer temperature) determines the binder's low temperature true grade. ΔT_c is a measure of how close the stiffness and m-value parameters are to each other with respect to their influence over the low temperature true grade. The revision to ASTM D7643 (2010) describes the process for selecting the low temperature true grade and defines ΔT_c .

Anderson et al. (2011) looked further into ΔT_c when they studied airfield pavements with the objective of predicting when preventative maintenance was needed to minimize the effects of non-load related cracking. Both transverse and block cracking occur due to environmental conditions (non-load related), such as low temperature and aging respectively. In other words, block cracking occurs on pavements that are older, while transverse cracking happens when the temperature first drops during winter. Thus, binder was aged 20, 40, and 80 hours to investigate the aging effects at low temperatures, not necessarily correlated to any particular service life (Anderson et al., 2011). Their work on cracking was based on concepts developed by Glover et al. (2005).

Glover et al. (2005) relates cracking behavior to ductility at low temperatures. They used the Maxwell element to better understand rheological properties of binders, in turn characterizing changes in ductility. Glover et al. (2005) found that ductility testing has low repeatability and required an additional piece of equipment, so they developed a new parameter. The parameter $\frac{G'}{\eta'}$ is inversely related to ductility in a log-log plot, quantifying the loss of flexibility with aging. G' represents the storage modulus and η' the dynamic viscosity. As $\frac{G'}{\eta'}$ increases, ductility decreases. In order to calculate $\frac{G'}{\eta'}$, the Dynamic Shear Rheometer (DSR) was run at 10 rad/s and 44.7°C to simulate ductility at 15°C and 1 cm/min. Glover et al. (2005) determined a cracking warning of 3 kPa/s (5 cm for ductility) and a cracking limit of 0.9 kPa/s (3 cm for ductility).

Anderson et al. (2011) used the findings of Glover et al. (2005) to further relate ductility and ΔT_c . They found that as the stiffness decreases on a m-controlled binder, the low temperature true grade also decreases because the m-value and stiffness both contribute to the binder gaining relaxation. Binder oxidation over time exhibits the same trend but in the

opposite direction, showing an increase in the low temperature grade as the binder ages. But, there is a faster loss of relaxation properties (m-value) relative to stiffness because m-value and stiffness are not linearly related. Therefore, the difference between T_c based on m-value and stiffness widens as the binder ages, producing a larger ΔT_c . Anderson et al. (2011) defines a cracking warning of 2.5°C and a cracking limit of 5°C. Using this knowledge of ΔT_c and ductility, as ΔT_c increases, ductility decreases. They verified this correlation using field and lab data, producing a consistent trend, though not linear. Therefore, according to Anderson et al. (2011), either $\frac{G'}{G''}$ or ΔT_c can be used to predict asphalt pavement cracking behavior. Regardless, both of these indicators improve upon the current system of using the BBR to characterize low temperature cracking behavior.

1.2.4 Summary of Performance Characteristics in the PG System

The PG system was a huge step forward from penetration grading and AR and AC viscosity grading systems. It moved from a highly empirical to a performance-based system with the goal of creating a system applicable to any climatic conditions and varying asphalt binder sources. The main focus of all of the systems has been to best replicate field performance based on a laboratory measured parameter. Each grading system has moved closer to this goal, but it has yet to be achieved.

One of the main reasons why the PG grading system needs alterations is due to the introduction of additives and modifiers. Different chemicals are added to asphalt binders to meet the required PG specification, but the desired performance is not adequately measured by the current specification. When the PG grading system was created, modified binders did not exist so they were never considered. Thus, the current PG specification needs an upgrade to account for both unmodified and modified binders in the design of all the test methods. Much research has been conducted to improve upon the current Superpave methods. New test methods have been developed such as MSCR for high temperatures, poker chip for intermediate temperatures, and ΔT_c for low temperatures. Nonetheless, the current PG grading cannot simply be eliminated; investigation must continue before these new methods replace different aspects of the PG grading system.

1.3 MOTIVATION

Further investigation must be done into the various new methods and parameters that seek to improve the current PG grading specification such as MSCR, poker chip, and

ΔT_c . As mentioned previously, substantial research has already been done proving strong correlations between these new test methods and different pavement failures individually but not as a whole. A corollary to this is that binders graded to be similar based on the current PG framework may result in vastly different field performances, owing to the differences in their chemical composition, processing methods used to produce the binder, and/or chemical or polymer modifiers added to the asphalt binder during and after binder production.

As a first step to improve the binder PG specification, this study examines the performance of several asphalt binders using the PG framework, as well as tests and parameters that may be potentially more sensitive to binder performance. The scope of this study is limited to the source and PG grade of the asphalt binders tested as well as the particular tests conducted. The results from this study cannot yet be extrapolated to all binders in general, but will hopefully in the future with the addition of more asphalt binders being tested. It must be emphasized that while this study recognizes the importance of binder properties, ensuring a good quality binder is necessary but not sufficient to ensure a good performance pavement.

CHAPTER 2. MATERIALS, METHODS AND PARAMETERS

2.1 MATERIALS

A total of 34 asphalt binders were used in this study from 12 different binder sources and 7 producers. All of the binders were sampled from the Texas Department of Transportation after undergoing the standard PG grading tests. The binder grades varied from a high temperature PG grade of 76 down to 58, while the low temperature PG grades ranged from -28 up to -22. Such a wide range of asphalt binder PG grades were tested to establish a complete understanding of the PG grading system, while ensuring that the most commonly used binder grades in Texas were more heavily represented.

The most prevalent binder grade used was PG 64-22 with 11 binders tested. PG 64-22 is the most common binder PG grade used in Texas. As such, this grade was sampled from several different sources. The next most common were PG 70-22 and PG 76-22 with seven binders each. Texas often sees higher PG binder grades than the rest of the United States due to the warmer weather, especially in the summer months. In fact, extreme fluctuations in temperature are often even seen on a daily basis, warranting a more balanced and rational PG approach. Grade bumping due to high traffic conditions leads to a higher than average PG high temperature binder grade. PG 58-22 had four sources that were tested, while PG 64-28 had only two sources that were tested during this study. Lastly, only one binder was tested from each PG grade of 58-22, 70-28, and 76-28 since these binder grades are uncommon in Texas. See Figure 2.1 for a graphical representation.

2.2 PG TESTS

Standard PG system tests were conducted following AASHTO M320. In order to achieve aging conditions, the Rolling Thin Film Oven (RTFO) and Pressure Aging Vessel (PAV) were used, following ASTM D2872 and D6521 respectively (Figures 2.2 and 2.3). On the high temperature side, the Dynamic Shear Rheometer (DSR) was used to find $\frac{G^*}{\sin \delta}$ on original and RTFO-aged binder at 10 rad/s (Figure 2.4).

The binders were tested at three temperatures (6°C above the labeled PG grade, 6°C below the labeled PG grade, and at the labeled PG grade). The same process was completed for both original and RTFO-aged binder, following ASTM D7175. In order to find a linear relationship between $\frac{G^*}{\sin \delta}$ and temperature, a log-linear plot was created. Figure 2.5 shows

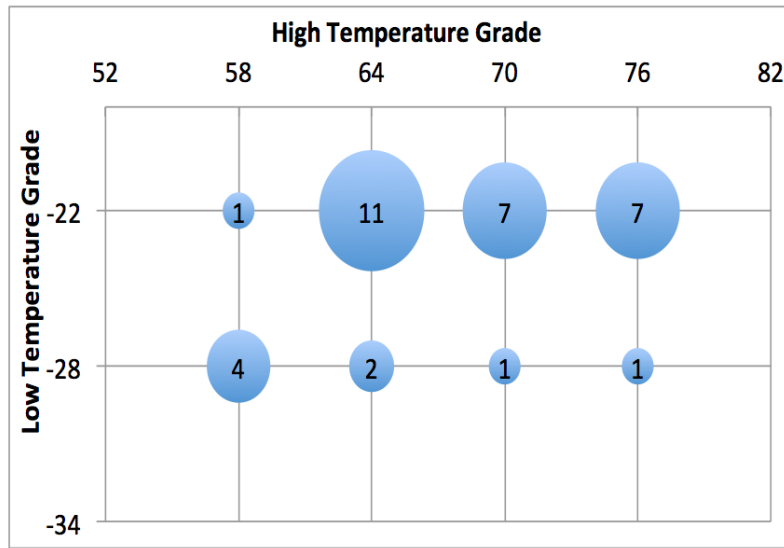


Figure 2.1. The PG grades of all the binders used in the study.

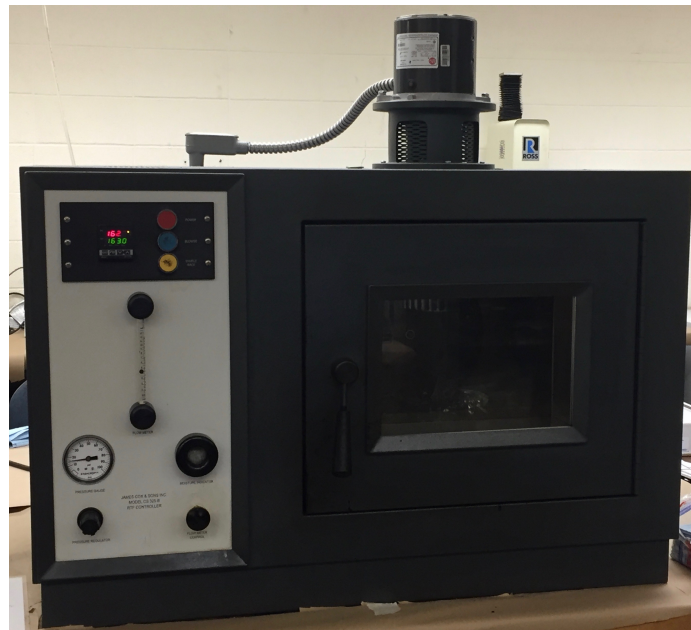


Figure 2.2. The James Cox & Sons Rolling Thin Film Oven, Model CS 325.

an example of this relationship for RTFO-aged binder E 64-22.

Then using the model of $\frac{G^*}{\sin \delta}$ versus temperature, the true temperature grade was determined based on a minimum value for $\frac{G^*}{\sin \delta}$ since the lower the $\frac{G^*}{\sin \delta}$, the softer the binder and more prone to rutting. The original binder true grade corresponds with a minimum cut-

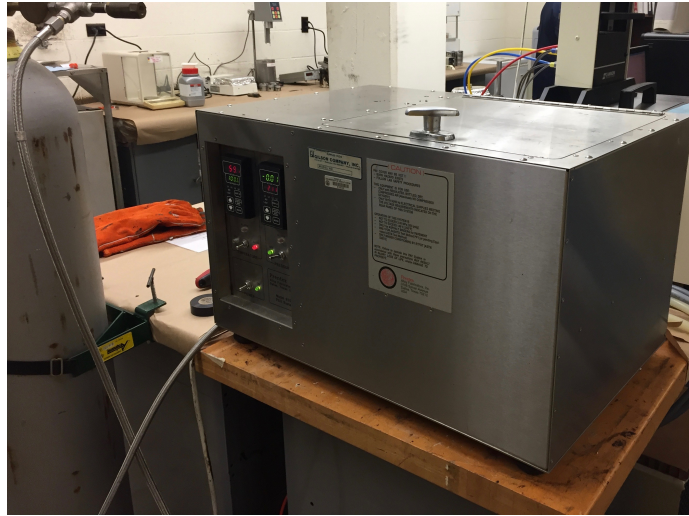


Figure 2.3. The Prestex Pressure Aging Vessel by the Gilson Company.

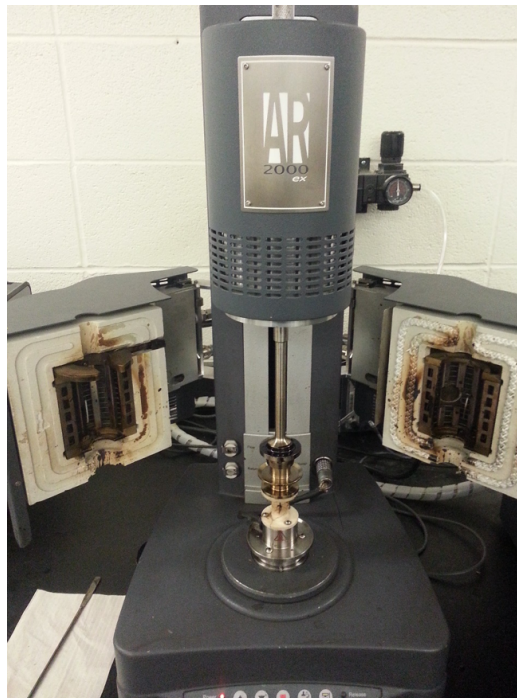


Figure 2.4. The AR 2000 Dynamic Shear Rheometer.

off value for $\frac{G^*}{\sin \delta}$ of 1 kPa, while the RTFO-aged true grade matches with a minimum value of 2.2 kPa for $\frac{G^*}{\sin \delta}$ according to AASHTO M320. The lower of the two true grades is rounded down to the nearest label (e.g. 58, 64, 70, 76) to produce the high temperature PG grade.

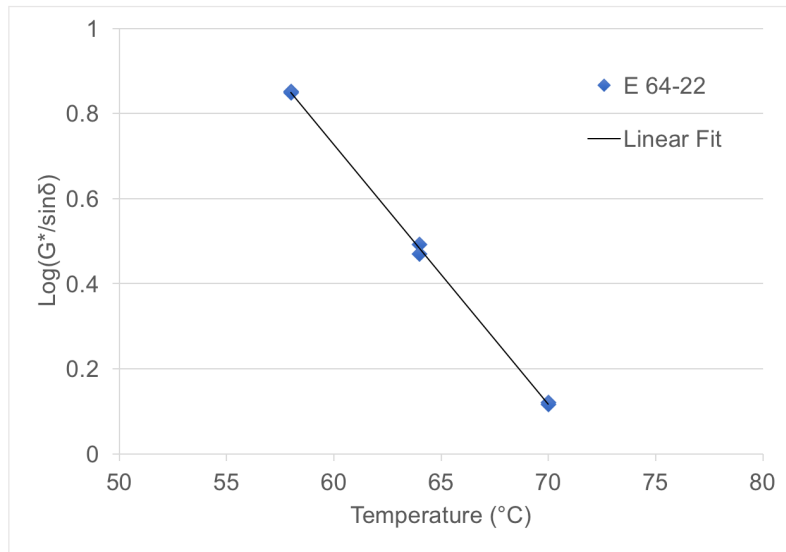


Figure 2.5. A log-linear plot of $\frac{G^*}{\sin\delta}$ versus temperature for RTFO-aged binder E 64-22.

On the low temperature side, Bending Beam Rheometer (BBR) testing was performed according to AASHTO T313 to determine the stiffness and m-value of each asphalt binder (Figure 2.6). Beams were molded to the size of 6.25 X 12.5 X 127 mm. The actual span length used for calculations is 101 mm because the beam slightly hangs off both supports in order to stay in place during testing. All binders were tested at three temperatures near 10°C warmer than the low temperature PG grade (4°C above, 10°C, and 16°C above the labeled PG grade) to shorten testing time. For example, a PG low temperature grade of -22 was tested at -18°C, -12°C, and -6°C. Beams were conditioned in a methanol bath for one hour before testing. A 100 g single-point mid-span loading was applied over a four-minute time period to PAV-aged binders.

The resulting m-value and stiffness at each of the three temperatures were used to create a relationship between the temperature and m-value, as well as the temperature and stiffness. A semi-log plot of stiffness versus temperature produced a linear relationship, while a plot of m-value versus temperature also created a linear relationship. Figures 2.7 and 2.8 display examples of these relationships for binder D 76-22.

These models were then used to back calculate the temperature at the specified m-value and stiffness occurring 60 seconds into the test. For m-value, a minimum value of 0.3 is specified in AASHTO M320. Since the m-value is the slope of the stiffness relationship at 60 seconds into the test, it indicates the ability of the binder to relax at low



Figure 2.6. The CANNON Instrument Company Bending Beam Rheometer (BBR), Model TE.

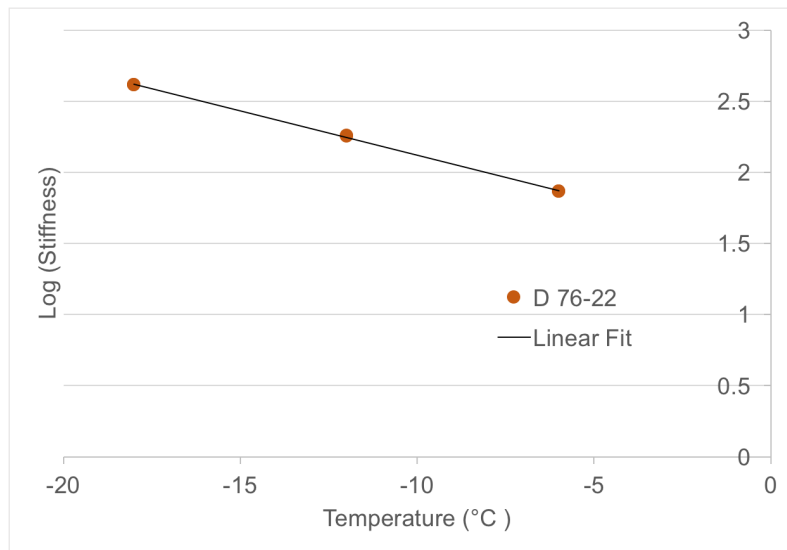


Figure 2.7. A log-linear plot of stiffness versus temperature for binder D 76-22.

temperatures. The minimum value ensures that the asphalt binder can relax at least the specified amount, even at low temperatures. For the stiffness, a maximum value of 300 MPa ensures that the binder does not become stiffer than 300 MPa at low temperatures. These parameters were used to determine the low temperature PG grade for each asphalt

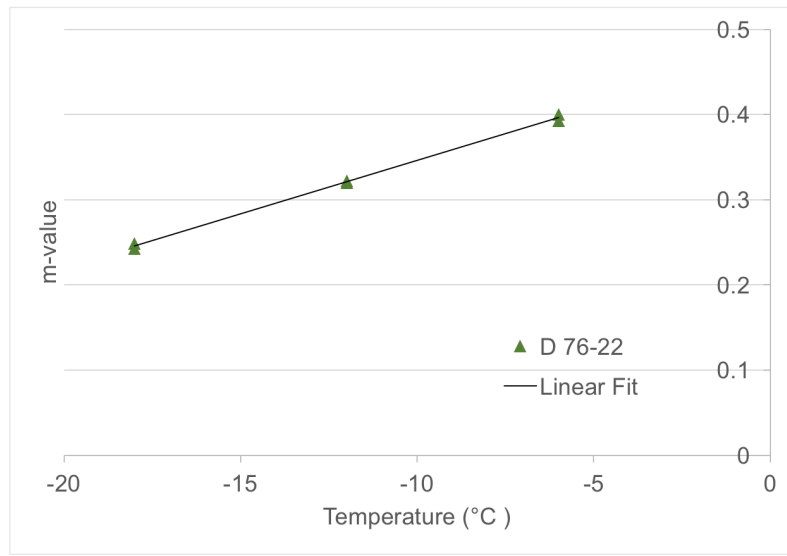


Figure 2.8. A linear plot of m-value versus temperature for binder D 76-22.

binder. The higher of the two temperatures, one based on m-value and the other based on stiffness, determines the low temperature true grade. Last, the true grade is rounded up to the nearest PG classification (e.g. -28, -22, -16) to result in the low temperature PG grade.

2.3 ADDITIONAL TESTS AND PARAMETERS BEYOND PG SPECIFICATIONS

Tests outside of the PG specification were run to better characterize asphalt binders of all PG grades. Binders that have the same PG grade do not necessarily behave the same in the field. Additional tests are meant to improve the current system of classifying asphalt binders. These tests executed outside the PG specification include: X-ray fluorescence spectrometry (XRF), Multiple Stress Creep Recovery (MSCR), spot test, poker chip, and BBR Pro; each of which will be described in greater detail in this section.

2.3.1 Metal Content

X-ray fluorescence spectroscopy (XRF) is a semi-quantitative analysis technique to detect various elements, typically from Sodium to Uranium on the Periodic Table (Arnold and Shastry, 2015). A hand-held X-ray fluorescence spectrometer was used to identify different materials in the original asphalt binders (Figure 2.9). Asphalt binder was heated and poured into a container before being placed upside down on the contact surface at the top of the machine. A benefit of this technique is the small amount of sample preparation

required.

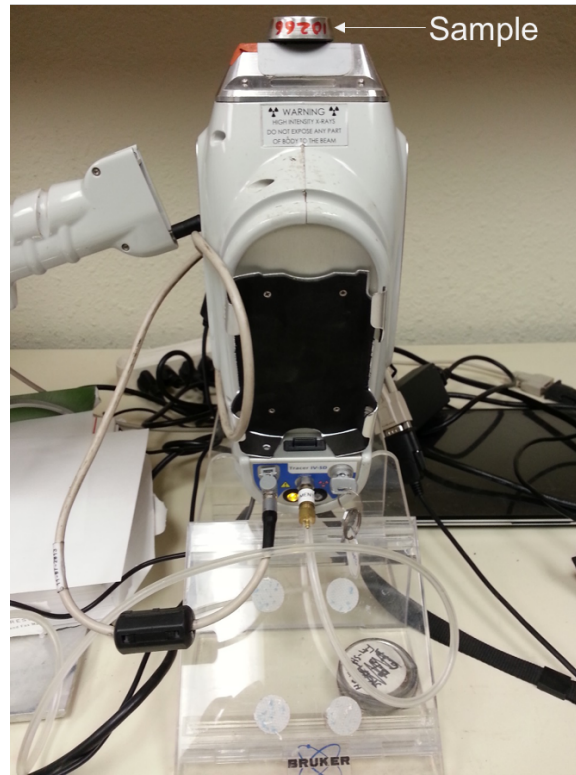


Figure 2.9. The Bruker X-ray fluorescence spectrometer.

The XRF procedure produces a spectra with various peaks, indicating the presence of different metals. The goal was to detect different asphalt modifiers in the asphalt binders by distinguishing the materials that make up the known modifiers. XRF can potentially be used to identify Polyphosphoric Acid (PPA), Recycled Engine Bottoms (REOB), and Crumb Rubber Modified (CRM) in original binders. REOB is of particular interest due to performance concerns especially at low temperatures (Arnold and Shastry, 2015). Table 2.1 shows the materials that correlate with specific modifiers added to binders.

Table 2.1. All the metals in each asphalt modifier (Arnold and Shastry, 2015).

	P	Ca	K	Fe	Ti	Cu	Br	Pb	Zn	Mo	Sn
PPA	X										
REOB	X	X		X					X	X	X
CRM		X	X	X	X	X	X	X	X		

Each additive has signature metals that will appear in the XRF spectra if present.

However, many asphalt binders already may have trace amounts of one or more of these metals. In addition, many of the metals that occur in one modifier are also present in another, so determining which modifier was added to a particular asphalt binder is difficult. Arnold and Shastry (2015) found that sometimes XRF can distinguish a relative difference between two asphalt binders or indicate an asphalt source but an objective and quantitative characterization is hard to accomplish due to the vast amount of variables (e.g. the type and concentration of metals may vary from one REOB source to another).

2.3.2 MSCR-Based True Grade

The Multiple Stress Creep Recovery (MSCR) test was conducted according to AASHTO M332. For the PG grading specification, original and RTFO-aged asphalt binders were tested in the DSR to find $\frac{G^*}{\sin \delta}$. The MSCR test replaces the RTFO-aged portion of testing for the PG specification, but still uses the $\frac{G^*}{\sin \delta}$ parameter for the original binder. MSCR measures the non-recoverable compliance, also known as elastic recovery, referred to as J_{nr} . J_{nr} is the non-recoverable strain at the end of a 9-second recovery period, followed by a 1-second loading period. Twenty cycles were applied at a shear stress of 0.1 kPa, followed by 20 more cycles at 3.2 kPa at the same three temperatures as for the standard high temperature PG grade testing. The average J_{nr} was calculated for each cycle before the average was taken of all 20 cycles at the particular applied shear stress. To find the J_{nr} for each cycle, the non recoverable shear strain was divided by the applied shear stress as shown in Equation 2.1.

$$J_{nr} = \frac{\text{Non-Recoverable Shear Strain}}{\text{Applied Shear Stress}} \quad (2.1)$$

The non-recoverable shear strain is the initial shear strain at the beginning of the creep subtracted from the final shear strain at the end of the recovery, presented in Equation 2.2. Figure 2.10 shows the non recoverable shear strain graphically for binder J 70-22. Only the first cycle is plotted as an example.

$$\text{Non Recoverable Shear Strain} = \text{Final Shear Strain} - \text{Initial Shear Strain} \quad (2.2)$$

The calculated J_{nr} at a stress level of 3.2 kPa is then used to find the high temperature true grade. (The J_{nr} determined at the stress level of 0.1 kPa will be used for the stress

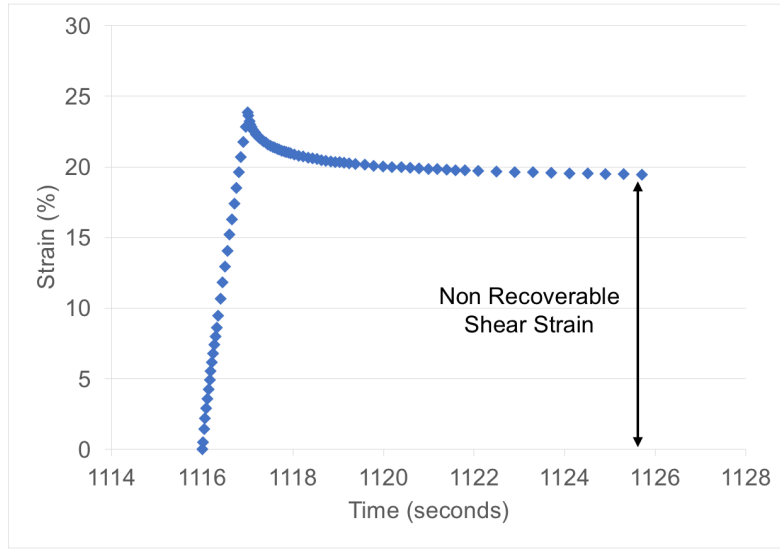


Figure 2.10. The percent strain over time of binder J 70-22 for the first cycle.

sensitivity parameter described later.) The higher the J_{nr} , the more permanent deformation so a maximum value is set based on the traffic level. For standard traffic, 4.5 kPa^{-1} is the cut-off while for heavy, very heavy, and extreme traffic conditions the maximum J_{nr} is 2, 1, and 0.5 kPa^{-1} respectively. In order to find the relationship between J_{nr} and temperature, a log plot is created using the J_{nr} found at three temperatures and two replicates. An example of this relationship is shown in Figure 2.11.

This model is used to back calculate the temperature at the maximum value for J_{nr} (e.g. 4.5 kPa^{-1} for standard vehicular traffic). Because this method adjusts the maximum J_{nr} based on the traffic conditions, grading bumping is not necessary. Note that in this study the true grade based on J_{nr} was determined and evaluated on its own for RTFO-aged binders. According to AASHTO M332 specification, the grade of the binder is determined using the more conservative temperature grade between $\frac{G^*}{\sin \delta}$ measured using original binder and J_{nr} measured using RTFO-aged binder. Arega et al. (2016) has shown that in most cases, the original $\frac{G^*}{\sin \delta}$ grade is more conservative and as such the J_{nr} does not dictate the grade of the binder .

The MSCR test can also be used to find the stress sensitivity of each asphalt binder. As mentioned in the previous chapter, polymer modifiers can cause a non-linear strain response and are sensitive to the stress level applied during the test. Therefore, a comparison of the J_{nr} values at each shear stress is important to ensure that the two values do not vary significantly, which is deemed over 75%. Equation 2.3 was used to calculate the stress

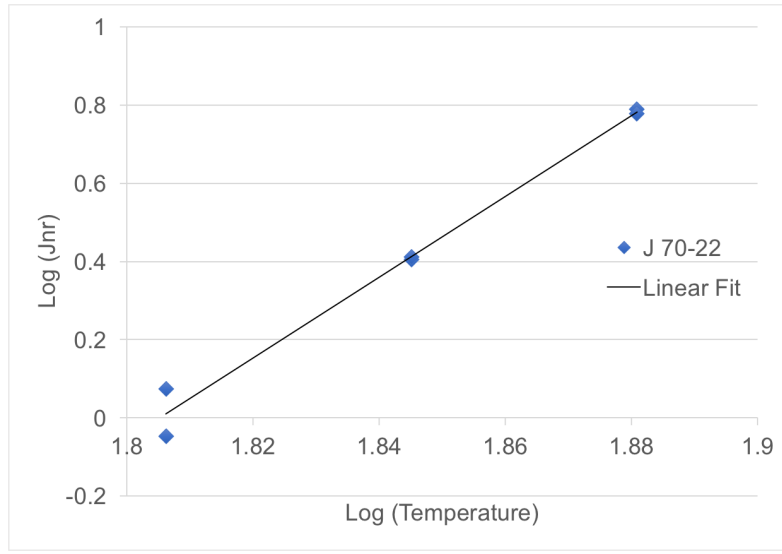


Figure 2.11. A log plot of J_{nr} versus temperature for binder J 70-22.

sensitivity of each asphalt binder. If the stress sensitivity falls below 75%, then the binder passes the stress sensitivity check.

$$\text{Stress Sensitivity} = \frac{J_{nr,3.2\text{kPa}} - J_{nr,0.1\text{kPa}}}{J_{nr,0.1\text{kPa}}} \leq 0.75 \quad (2.3)$$

2.3.3 Spot Test

The spot test originally began as an indicator of Thermal Cracked Residues (TCR) in 1933. TCR used in asphalt pavements in the 1920s and 1930s showed unacceptable age hardening leading to premature failures. Thus, the spot test was born. In fact, as of 1992, eight states still required the spot test, but the majority of states used the RFTO as a more accurate predictor of age hardening (Root and Moore, 1992). The spot test can also be used to determine if the asphalt binder has been overheated. In this study, the spot test was used to indicate the compatibility of the components of an asphalt binder (e.g. modifiers and original binder). The spot test was conducted according to AASHTO T102, but toluene was used instead of naptha standard. Two grams of binder were dissolved into 10 mL of toluene. Then, a drop was placed in the center of filter paper using a pipette (Figure 2.12).

The percent area on the black spot was compared to the total spot using the software ImageJ. The spots were imported into the computer via scan before being converted to grayscale. Once in grayscale, ImageJ was used to find the total black spot area and the

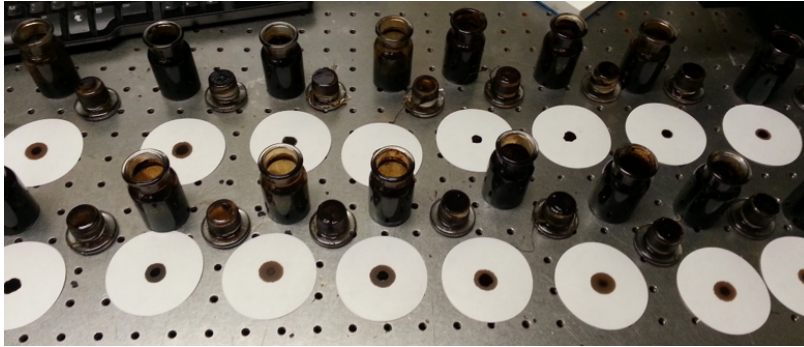


Figure 2.12. The dissolved binder beside the marked filter paper.

total spot area to find the percent black spot area. Figure 2.13 shows the spots as they go through the process. A homogeneous ring indicated good compatibility of components in the asphalt binder, while a solid ring indicated separation as shown in Figure 2.14.

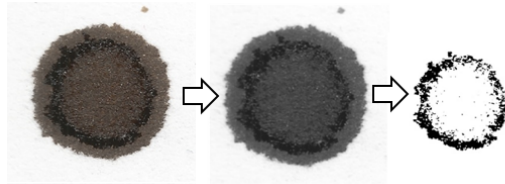


Figure 2.13. Spots at various steps of the process from scan to grayscale to ImageJ.

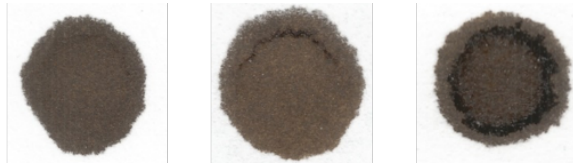


Figure 2.14. The different degrees of separation from homogeneous to separated.

2.3.4 ΔT_c

Finding the parameter ΔT_c does not require any additional testing beyond the standard BBR test already run to determine the low temperature PG grade, only additional calculations. As mentioned, for the PG low temperature grade, the higher (less negative) true grade based on the stiffness and the m-value determines the grade. For ΔT_c , the true

grade values from stiffness and m-value are subtracted to find the difference between the two parameters following ASTM D7643, shown in Equation 2.4.

$$\Delta T_c = \text{Temperature}_{\text{m-value}} - \text{Temperature}_{\text{stiffness}} \quad (2.4)$$

Calculating ΔT_c is important because the parameter shows how close the stiffness and m-value parameters are to each other with respect to their influence over the low temperature true grade. As mentioned in the previous chapter, the m-value true grade often determines the low temperature PG grade so ΔT_c allows the comparison of these two parameters, which cannot be seen by simply looking at the low temperature PG grade.

2.3.5 Aging Sensitivity

The properties of asphalt binders change with age, gaining stiffness and losing the ability to relax over time. In order to quantitatively show the effect of age on asphalt binders, each binder underwent long-term aging using the Pressure Aging Vessel (PAV) twice. In this thesis, long-term aging the material one time is referred to as PAVI and after the second round of long-term aging, the aging is referred to as PAVII. After undergoing short-term aging in the RTFO, ASTM D6521 was followed to age the material to reach PAVI. (PAVI is the same as PAV. The numeral was just added to prevent confusion with PAVII.) Then, the material was aged again using the PAV to reach PAVII. The only difference between PAVI and PAVII is that PAVII goes through the PAV process once more.

In order to determine the low temperature grade for the standard PG grading system, BBR was run on PAVI-aged binder as described previously. Thus, the only additional testing required was on PAVII-aged binders. As with the PAVI-aged binder, AASHTO T313 was followed; the only difference being that PAVII-aged binder was used. The binders were tested at three temperatures, the same as for the standard BBR test in order to make the comparison. The m-value and stiffness were gathered to compare the PAVI and PAVII binder properties. Equation 2.5 was used to calculate the difference between the two aging conditions for both m-value and stiffness separately.

$$\text{Percent Difference} = \frac{\text{PAVII} - \text{PAVI}}{\text{PAVI}} \times 100 \quad (2.5)$$

2.3.6 Strength Test at Intermediate Temperature

The current PG grading specification for intermediate temperature uses the DSR to measure $G^* \sin \delta$ at a maximum of 5,000 kPa for a frequency of 10 rad/s on PAV-aged asphalt binder. As described in the previous chapter, alternative methods have been developed to improve upon the current PG specification. The poker chip test utilizes a normal tension-compression universal loading frame (in the Instron E1000) to apply a constant stress increment of 1 N/sec until failure to RTFO-aged binder at 18°C. In order to determine the testing temperature, 300 cities across Texas were surveyed to find the average air temperature. Then, cities were grouped based on the PG grade that was most applicable. Lastly, the average air temperature was taken of each group to find the testing temperature for each particular PG grade (average temperatures were rounded to the nearest degree). It turned out that all binders used in this study should conduct testing at 18°C.

In order to control the temperature, a plastic chamber was installed around the Instron. A thin film of asphalt binder, about 300 μm , was sandwiched between two metal plates of diameter 14.6 mm. The samples were conditioned for 20 minutes in the temperature controlled chamber to reach equilibrium. The test setup is displayed in Figure 2.15 as well as a schematic of the plates in Figure 2.16. The detailed test procedure is outlined in Hajj (2016). The strength at failure was noted due to the tensile stress applied. All the asphalt binders with the same PG grade were compared.

2.3.7 Strength Test at Low Temperature

The standard BBR test used to find the PG low temperature grade does not measure strength of the asphalt binders, only the stiffness and relaxation (m-value). Thus, the BBR Pro (CANNON Instrument Company) was used to determine the strength of each asphalt binder at both PAVI and PAVII aging conditions. Figure 2.17 displays the machine used for testing.

AASHTO T313 was followed for beam preparation and conditioning in the bath, but a different load was applied. Instead of applying a constant load over the entire testing period, a constant rate of 4 N/min was used. The stress increment was applied until failure, which is the point at which the beam physically broke. The maximum stress (σ) was calculated at the maximum load (P) the beam could withstand using Equation 2.6. The thickness, width, and length of the all beams is the same as for the standard BBR test with the dimensions 6.32 X 12.6 X 100 mm used in Equation 2.6. (The beam length is actually

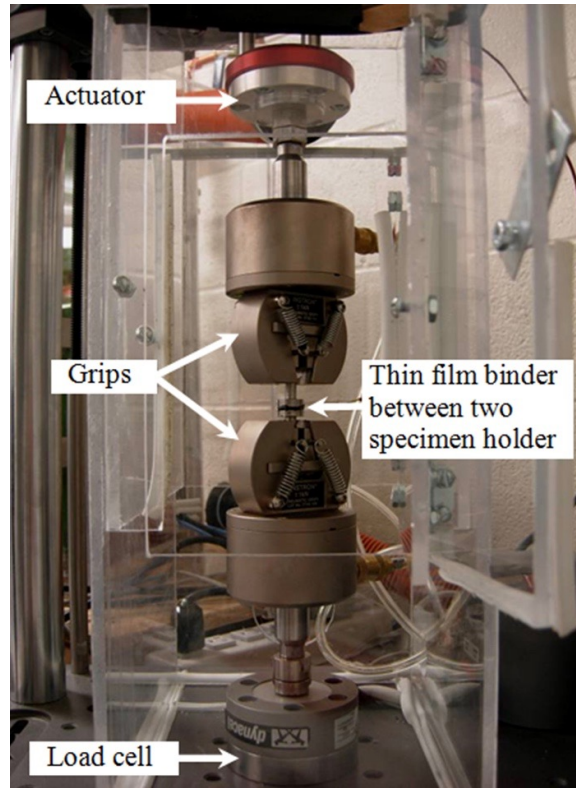


Figure 2.15. The Instron E1000 set up (Sultana, 2014).

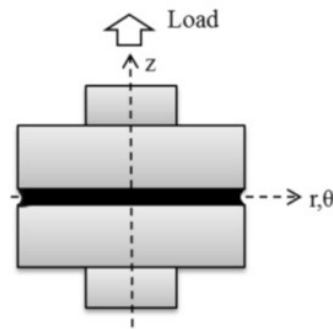


Figure 2.16. A schematic of the plate geometry (Sultana, 2014).

127 mm, but the span length is used since the distance between the two supports is the length of load applied.)

$$\sigma = \frac{3 \times P \times \text{Length}}{2 \times \text{Width} \times \text{Thickness}^2} \quad (2.6)$$

The asphalt beams were tested at two temperatures, 10°C above the low temperature

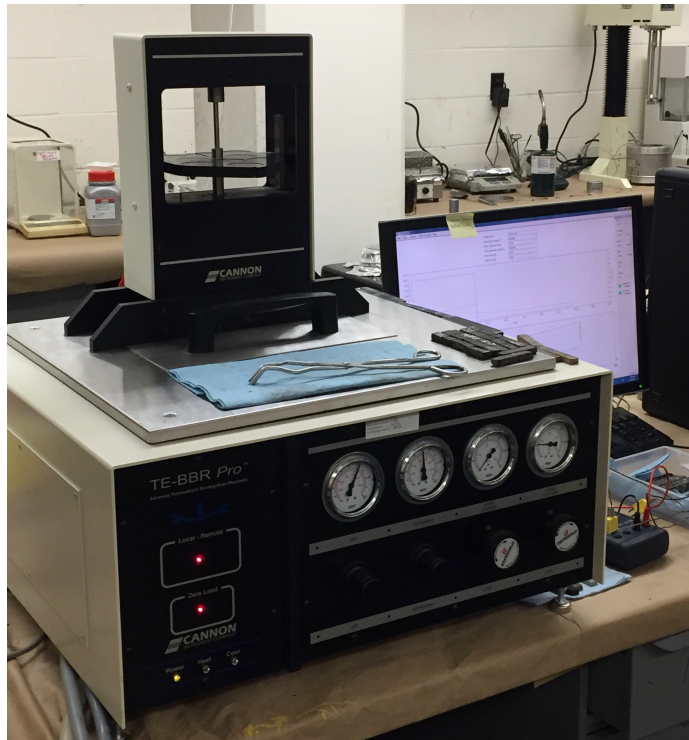


Figure 2.17. The CANNON Instrument Company Bending Beam Rheometer (BBR) Pro, model TE.

PG grade and 6°C below that temperature (4°C above the low temperature PG grade). In other words, low temperature PG -22 grade binders were tested at -12°C and -18°C , while the PG -28 binders were tested at -18°C and -24°C . The maximum stress of all the asphalt binders at both temperatures and aging conditions were compared.

CHAPTER 3. LABORATORY TESTING RESULTS

3.1 OVERVIEW

This chapter presents and explains the results from the various tests run that fall outside of the PG specification. But the current PG grading will still be used as a point of comparison between the current PG grading system and new test method results. The methods followed were explained in the previous chapter; only the results and analysis are presented in this chapter. The test results outlined include: XRF, MSCR, spot test, ΔT_c , aging sensitivity, poker chip, and BBR Pro.

3.2 LABORATORY TESTING RESULTS

For all of the graphs presented, each binder was given a letter identifier for the source followed by the labeled PG grade. Binders were labeled Source A through L. For example, J 70-22 represented Source J with a PG grade of 70-22. This grade was verified by the TxDOT laboratory before being received to undergo all testing. Outliers were defined differently for each test and based on a holistic view of the results. It must be noted that these outliers are not necessarily positive or negative properties; further work must be done to form such conclusions.

3.2.1 Metal Content

As mentioned in the previous chapter, each peak in any given XRF spectrum represents a different metal found in the original asphalt binder. The results from XRF are presented in Figures 3.1-3.6. Each asphalt modifier has a combination of these metals, as was presented in Table 2.1 from the previous chapter. A summary of these results is displayed in Figure 3.7. The blue represents binders where none of the four metals (iron, zinc, calcium, or phosphorus) were found, while gray represents binders that were not tested due to limited resources. If a box has multiple colors, then XRF indicated multiple metals present.

Each modifier has a signature combination of metals that indicate the presence of a particular modifier. Table 3.1 displays the binders in which metals were detected and the possible corresponding modifiers. There lies an issue in differentiating between modifiers since modifiers share metals. It was difficult to determine which modifier was added

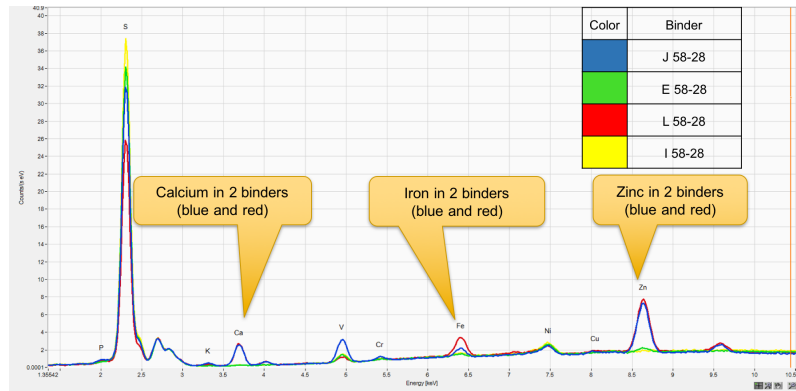


Figure 3.1. The XRF spectra for binders with a high temperature grade of PG 58.

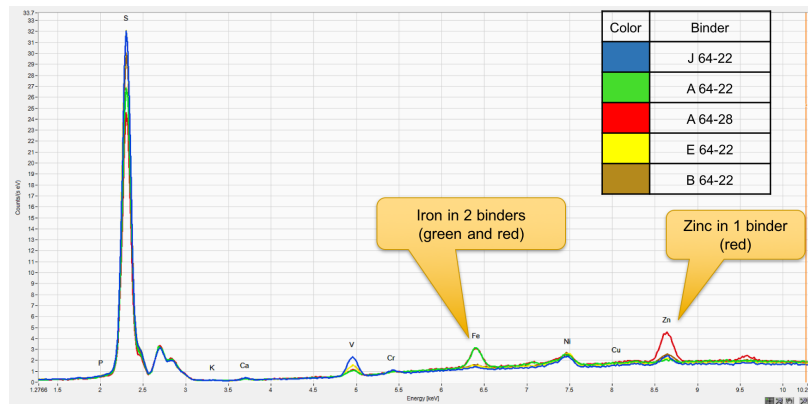


Figure 3.2. The XRF spectra for the first half of binders with a high temperature grade of PG 64.

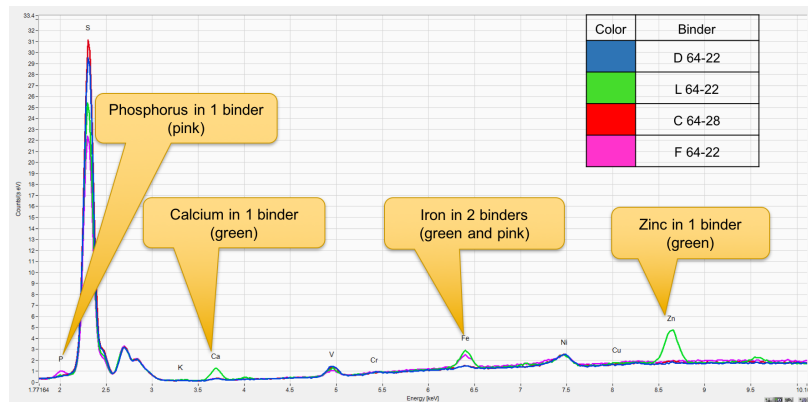


Figure 3.3. The XRF spectra for the second half of binders with a high temperature grade of PG 64.

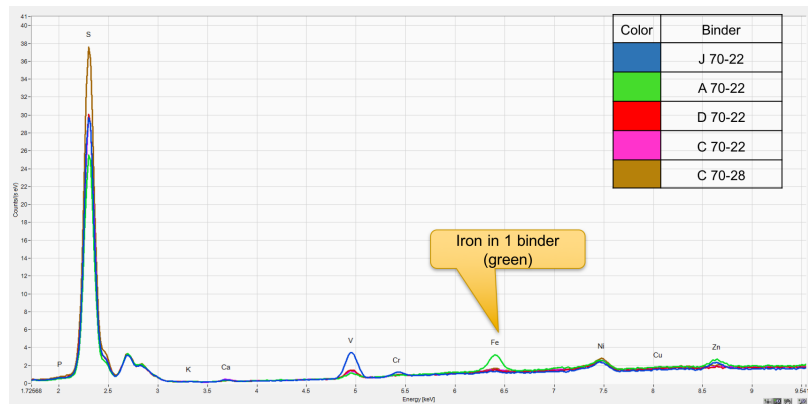


Figure 3.4. The XRF spectra for first half of binders with a high temperature grade of PG 70.

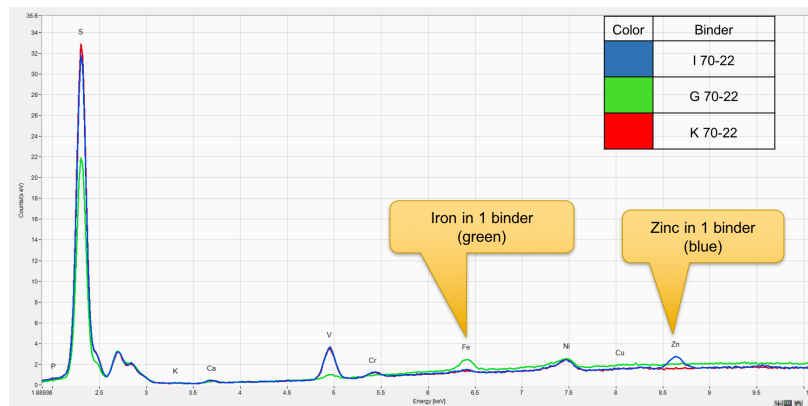


Figure 3.5. The XRF spectra for second half of binders with a high temperature grade of PG 70.

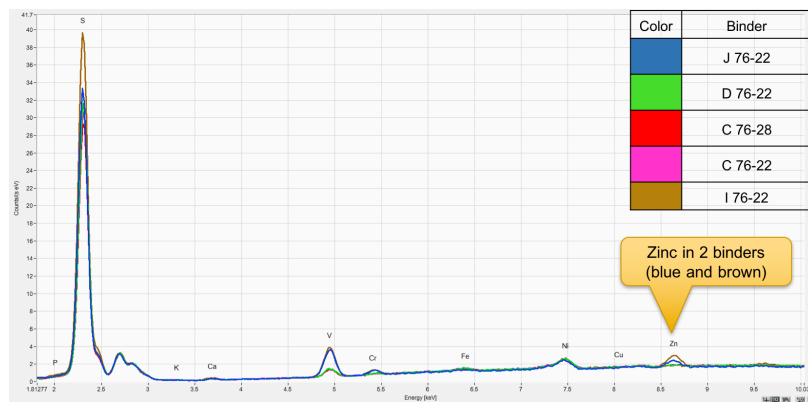


Figure 3.6. The XRF spectra for binders with a high temperature grade of PG 76.

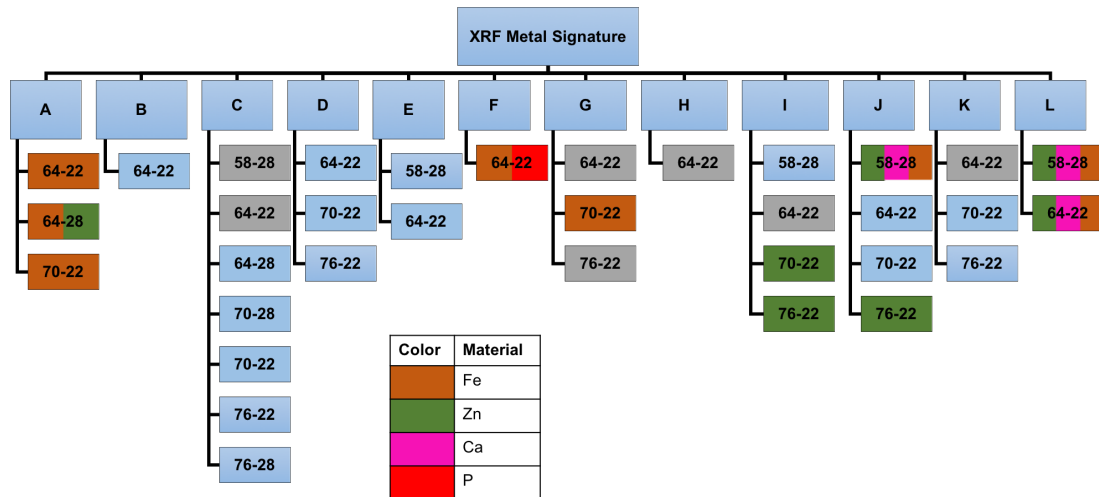


Figure 3.7. A summary of all the binders tested and the metals found through the XRF test.

with certainty. In addition, asphalt binders have metals present before modifiers are added depending on the source. For example, a particular source may have a large amount of phosphorus, while for another source calcium may be very prevalent. Therefore, a knowledge of the typical asphalt source properties is necessary along with more extensive XRF testing in order to confidently detect the presence of particular modifiers. Lastly, not all modified binders include metals so only speculation can be drawn. It should be noted that Table 3.1 is only a suggestion, not a correlation made with certainty; more information about the binder source metal composition is needed.

Table 3.1. The metals detected and the corresponding modifier.

Binder	Metal 1	Metal 2	Metal 3	Modifier
A 64-22	Fe	-	-	REOB or CRM
A 64-28	Fe	Zn	-	REOB or CRM
A 70-22	Fe	-	-	REOB or CRM
F 64-22	Fe	P	-	REOB
G 70-22	Fe	-	-	REOB or CRM
I 70-22	Zn	-	-	REOB or CRM
I 76-22	Zn	-	-	REOB or CRM
J 58-28	Zn	Ca	Fe	REOB or CRM
J 76-22	Zn	-	-	REOB or CRM
L 58-28	Zn	Ca	Fe	REOB or CRM
L 64-22	Zn	Ca	Fe	REOB or CRM

3.2.2 MSCR-Based True Grade

MSCR testing was conducted along with the standard high temperature PG testing in the DSR. The results of the MSCR test are compared to those obtained from the standard PG testing in Figures 3.8-3.11. As mentioned previously, $\frac{G^*}{\sin \delta}$ was used to find the true (also known as the continuous) grade for both original and RTFO-aged binders, while J_{nr} was the basis for the true grade of RTFO-aged binders. In order to best show in the difference in true grade, each graph shows the true grade based on the original $\frac{G^*}{\sin \delta}$, RTFO-aged $\frac{G^*}{\sin \delta}$, and MSCR testing. Note that based on the specification used, the actual true grade of the binder is the lower of the two values based on original and RTFO $\frac{G^*}{\sin \delta}$ or the lower of the two values based on original $\frac{G^*}{\sin \delta}$ and RTFO-aged J_{nr} from the MSCR test. However, in this case each of the three parameters is considered independently to compare the true grade.

The red solid line on each figure marks where the true grade exceeds the point at which it would round down to the labeled PG high temperature grade. For example, in Figure 3.9 binder A 64-28 has an MSCR true grade of 74, which rounded down to a high temperature grade of PG 70, not the labeled PG 64. In addition, some of the bars are filled in red to indicate outliers, which are so great that they reach far outside the range of the graph; in actuality the red bars stretch far above the shown maximum vertical axis true temperature grade. In other words, the red bars indicate true grades greater than 12°C (two PG grades) above the labeled high temperature grade. For instance, binder C 76-28 has an MSCR true grade of 89, which is 13°C above the labeled grade of PG 76. Figure 3.12 summarizes all of these results.

Same as Figures 3.8-3.11, red boxes indicate outliers by a difference in the true grade of greater than 12°C. In addition, the labeled grade underlined represents a true grade that was not only more than 12°C above the label grade of the binder, but also a true grade greater than 90°C, an extreme outlier. The outlier criteria was chosen since a 12°C difference would bump the grade up by two high temperature PG grades, making a significant impact on the final PG high temperature grade. There were a concentration of outliers from Source C that should be noted for comparison to other tests.

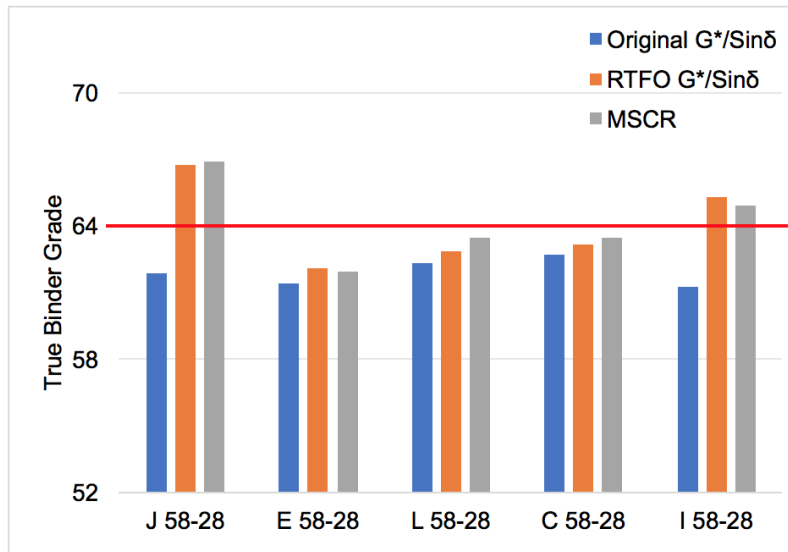


Figure 3.8. The true grades for all high temperature PG 58 binders.

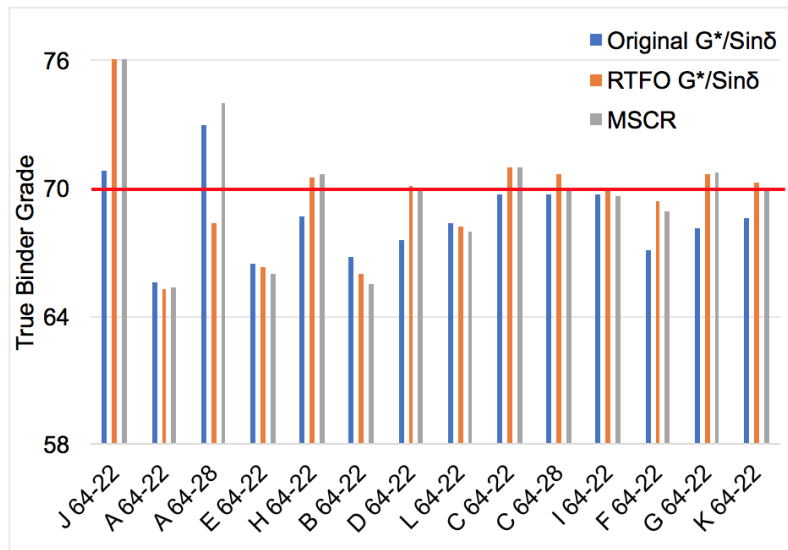


Figure 3.9. The true grades for all high temperature PG 64 binders.

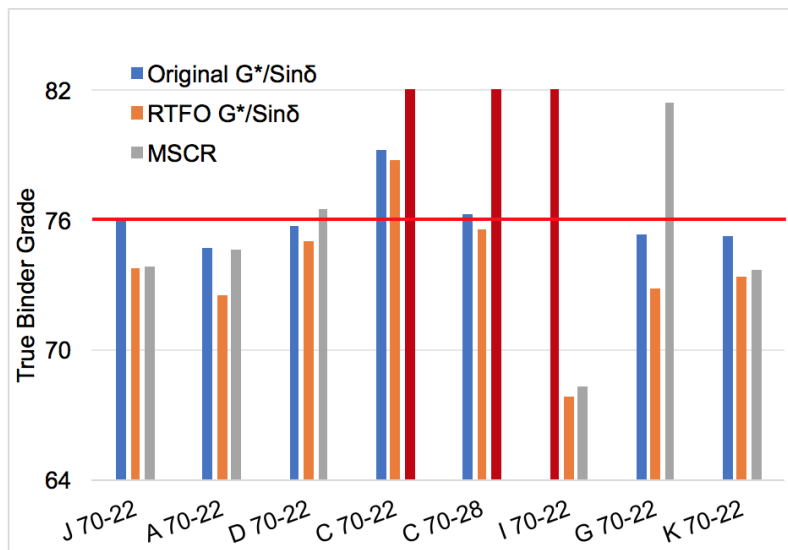


Figure 3.10. The true grades for all high temperature PG 70 binders.

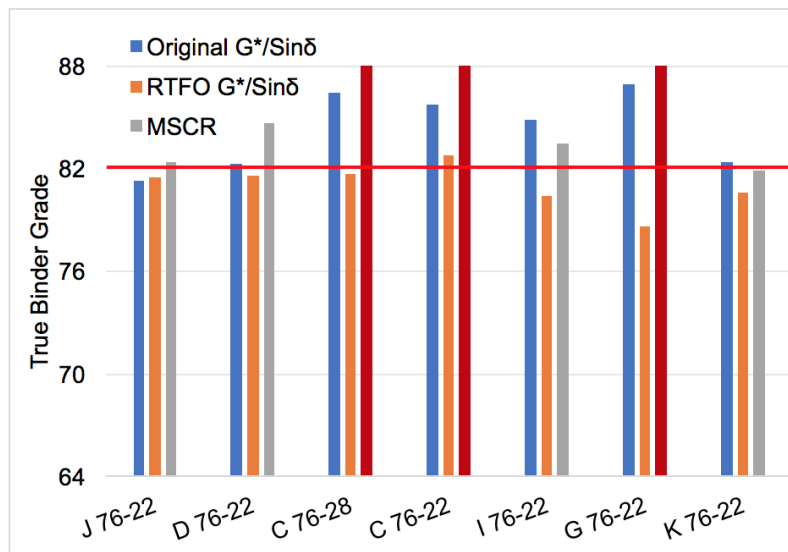


Figure 3.11. The true grades for all high temperature PG 76 binders.

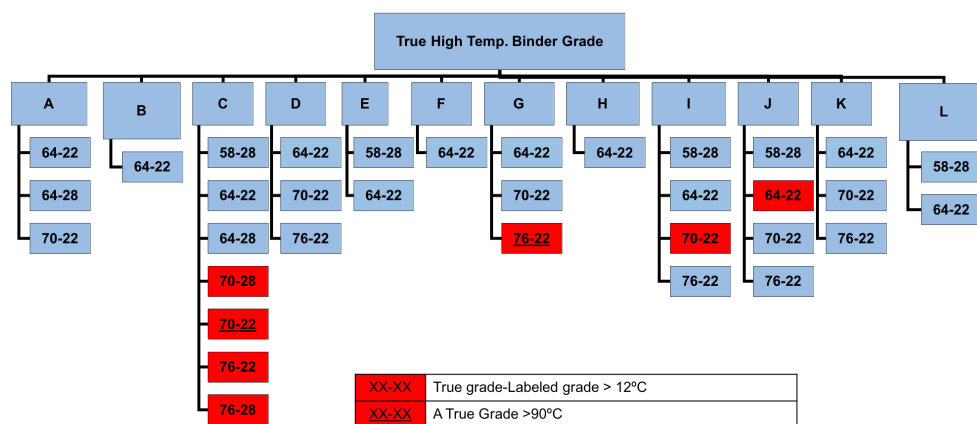


Figure 3.12. A summary of all the binders tested and outliers present for high temperature PG grading.

3.2.3 Spot Test

For the spot test, the software ImageJ was used to determine the percentage black area compared to the total area of the spot. Ideally, one would expect a homogeneous and uniform spot formation. In the case of binder with incompatible or unstable chemical fractions and/or modifiers, the spot has a distinct separation and is not homogeneous. REOB or CRM could potentially be correlated with an unstable modifier and thus show distinct separation, but not enough data was collected during the XRF testing to assuredly make the connection. The percentage black area was used as a quantitative measure for the separation when such separation did occur. Figures 3.13 and 3.14 show the spot test results in terms of black area out of the total spot area.

In each figure, the solid red line marks the 10% spot area boundary, above which outliers exist. Also, red bars represent extreme outliers that fall far outside the range of the other values since they have a spot area greater than 20%. It should be noted that the red bar extreme outliers stretch far beyond the maximum vertical axis range provided. Outlier criteria was determined upon inspection of the results. Since there are no current specification limits for these measurements, this criteria is only applicable to this study at this point in time. A summary of all the results is presented in Figure 3.15 with all the outliers in red and the extreme outliers underlined. Source C and I displayed a considerable amount of outliers.

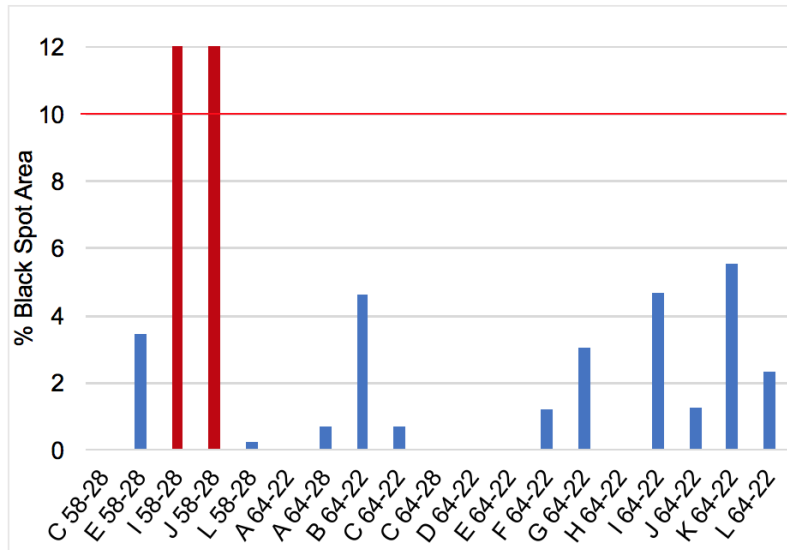


Figure 3.13. The percent black area for all high temperature PG 58 and PG 64 binders.

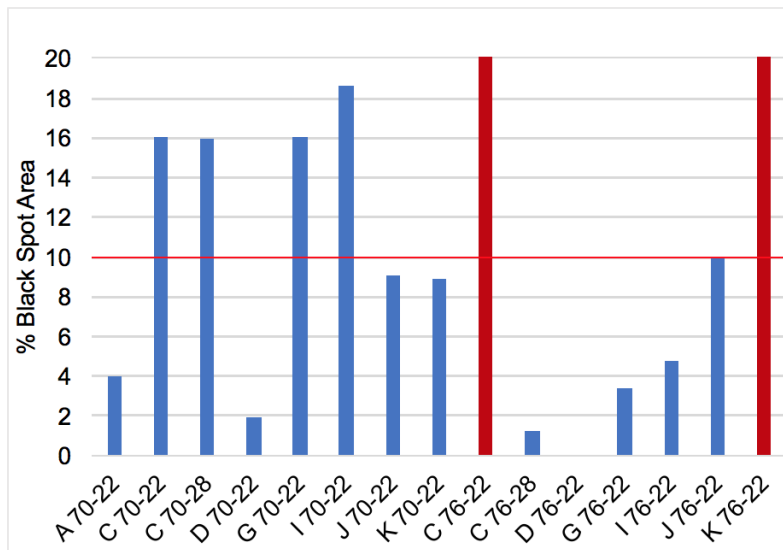


Figure 3.14. The percent black area for all high temperature PG 70 and PG 76 binders.

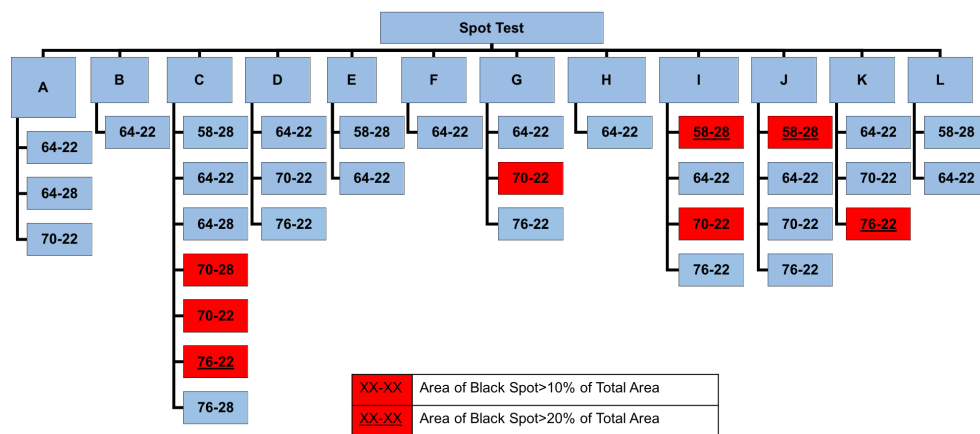


Figure 3.15. The results for percent black area of the total area with outliers in red.

3.2.4 ΔT_c

ΔT_c is not a separate test, but a calculation that looks at the difference between two true grades found from the BBR test, one based on the m-value and the other based on the stiffness for PAV-aged binders, presented in Figures 3.16-3.18. The final PG low temperature grade is the higher (less negative) of the two true grades rounded up to the nearest PG grade classification. For instance, binder A 64-28 has a m-value true grade of -20°C , while the stiffness true grade is -23°C . Picking the greater of the two, the low temperature true grade is m-value controlled with a value of -20°C that rounds up to -16°C for the PG grade with a ΔT_c of 3°C . But simply looking at the PG grade does not show whether it is m-value or stiffness controlled and the difference between the two values.

As mentioned in previous chapters, the PG low temperature grade is almost always m-value controlled as in the example. This raises concerns since only the relaxation and not stiffness properties at low temperatures are contributing to determining the low temperature grade. In fact, for this study only one binder was stiffness controlled, as indicated with a red bar in Figure 3.18, and just by 0.5%. It should be noted that not all the $\frac{G^*}{\sin \delta}$ values for the original and RTFO-aged binders met the 0.3 minimum (from AASHTO M320) when tested in the lab because the material underwent multiple rounds of heating before the standard PG high temperature testing.

Outliers in Figures 3.16-3.18 represent the ΔT_c values that were greater than 6°C , since 6°C is the difference between PG grades. (A red line on each graph at 6°C helps differentiate the outliers.) In other words, if ΔT_c is less than 6°C , it does not matter if the binder is m-value or stiffness controlled because the final PG low temperature grade would end up the same. But if ΔT_c is greater than 6°C , the PG grade is not taking into account both properties measured during the BBR test. Thus, binders are not required to follow maximum stiffness criterion, only minimum relaxation requirements since most binders are m-value controlled. Hence, the m-value controlled binders show potentially less sensitivity to temperature. Figure 3.19 displays a summary of the results with the outliers in red. In addition, the one binder that was stiffness controlled is underlined. It should be noted that the gray box indicates a binder that was not tested due to limited resources and time. There are a concentration of outliers from Source F, G, H and J.

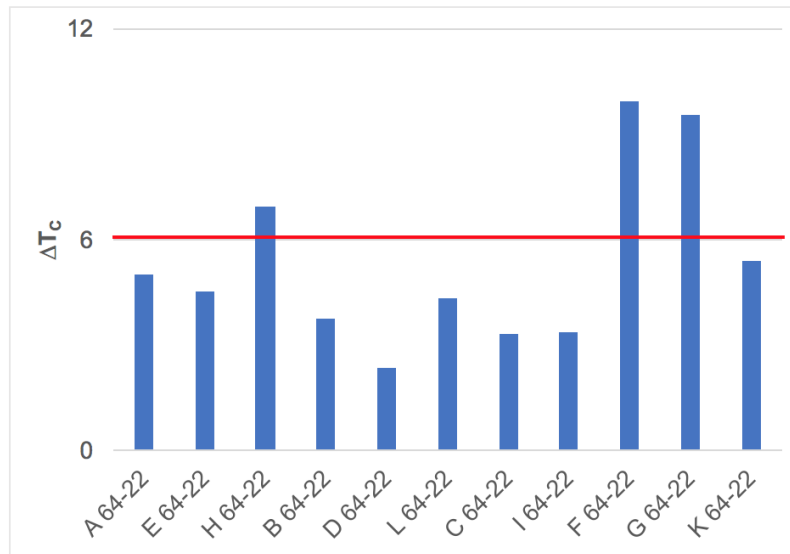


Figure 3.16. The difference in m-value and stiffness true grades for PG 64-22 binders.

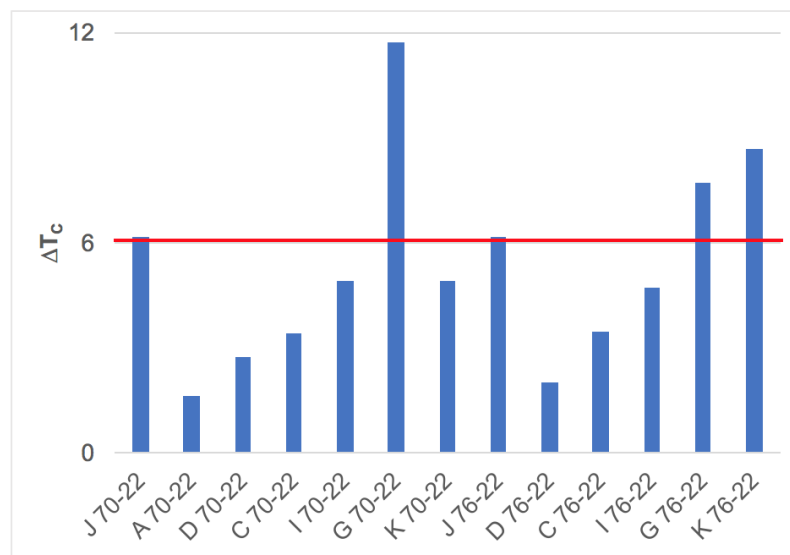


Figure 3.17. The difference in m-value and stiffness true grades for the remaining low temperature PG -22 binders.

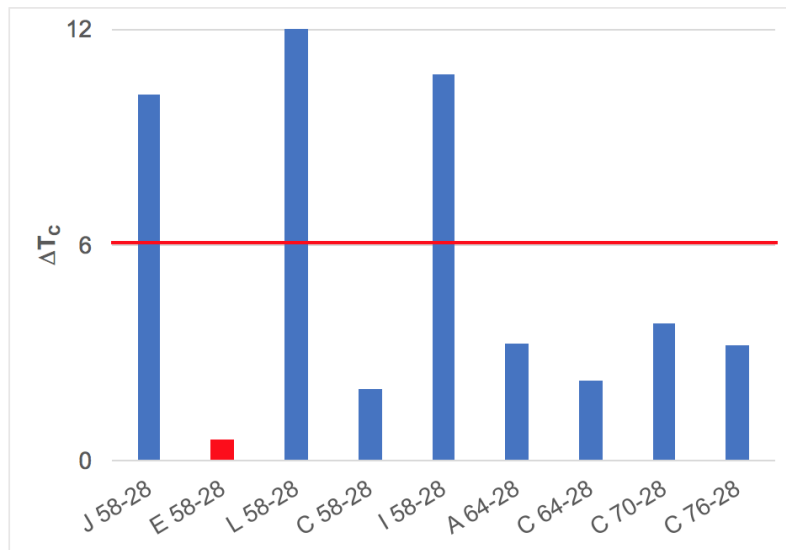


Figure 3.18. The difference in m-value and stiffness true grades for low temperature PG -28 grade.

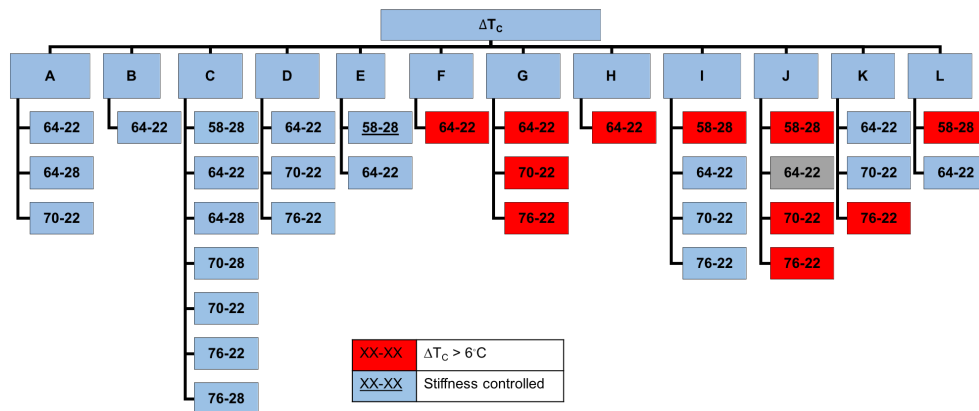


Figure 3.19. A summary of all the results for ΔT_c with outliers in red.

3.2.5 Aging Sensitivity

Asphalt binders underwent PAVI (generally referred to as PAV) and PAVII aging in order to compare the properties at the two aging conditions. Only PAVII aging was necessary beyond the scope of the PG specification, along with additional BBR testing on the further aged material. Both the m-value and stiffness were compared using Equation 2.5 from the previous chapter to find the percent difference. Figures 3.20-3.22 present the results of the comparison.

Outliers are defined as those less than -20% (larger negative) for m-value and greater than 40% for stiffness. The difference in m-value was a negative percentage since relaxation properties decrease with age, while stiffness of binders increases as time passes. A summary of the results is presented in Figure 3.23 with the m-value outliers in red and the stiffness outliers in brown. Boxes split with both colors indicate that the particular binder had both outliers, such as binder E 58-28. For simplicity of the m-value outlier criterion, the equivalent was used for the summary of the results (Figure 3.23) by flipping the inequality and taking away the negative. The outliers chosen follow no standard and only apply to the data set in this study; criteria was chosen based on observation of the results. Source K showed a large concentration of outliers.

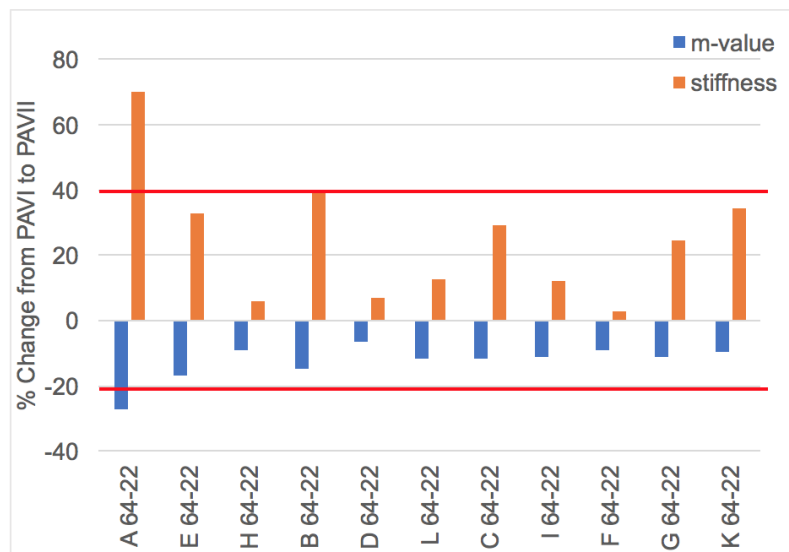


Figure 3.20. The change in m-value and stiffness between aging conditions for PG 64-22 binders.

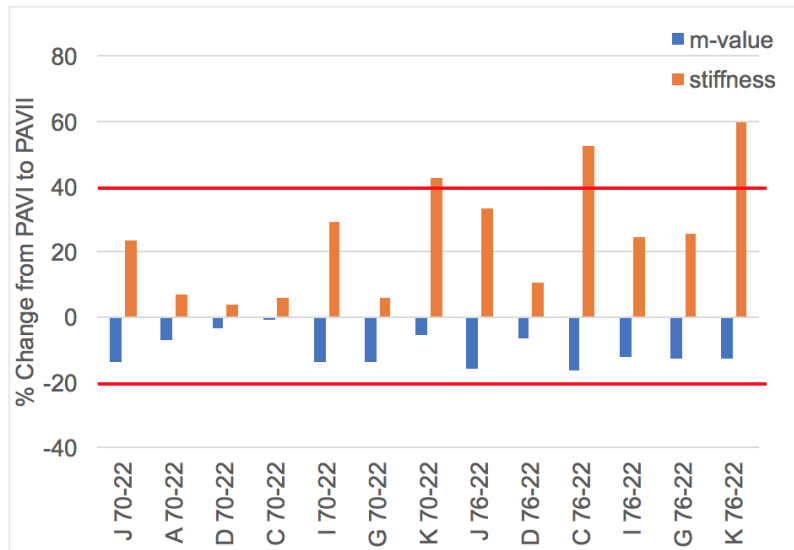


Figure 3.21. The change in m-value and stiffness between aging conditions for the remaining low temperature PG -22 grade binders.

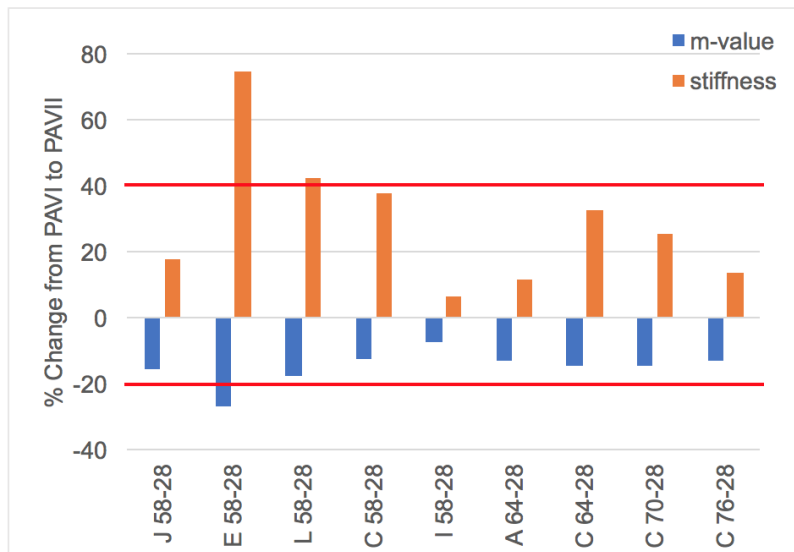


Figure 3.22. The change in m-value and stiffness between aging conditions for low temperature PG -28 grade binders.

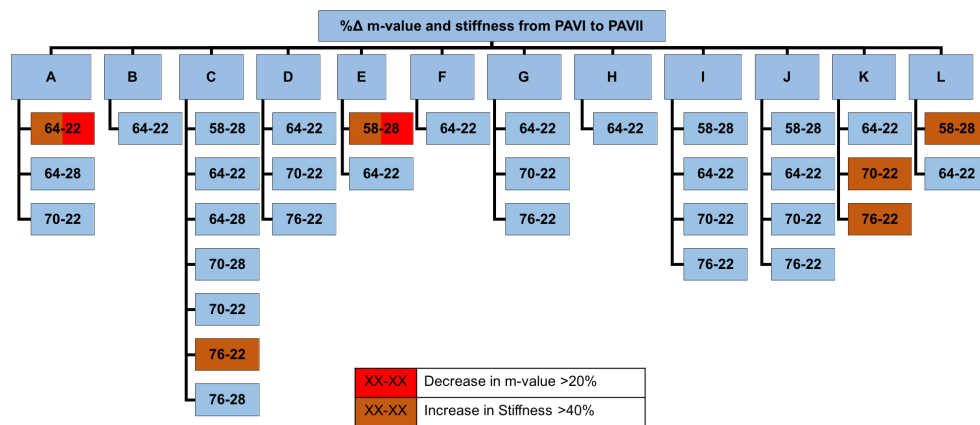


Figure 3.23. A summary of results for changes in low temperature properties with outliers in red and brown.

3.2.6 Strength Test at Intermediate Temperature

As mentioned in the previous chapter, the poker chip test was run on RTFO-aged binder at an intermediate temperature of 18°C and a loading rate of 1 N/sec. The tensile strength at fracture was collected for each binder. Because the intermediate properties of each asphalt binder depend on both the high and low temperature PG grade, the results are presented based on the PG grade. Binders C 70-28, C 76-28, L 58-22 were not plotted since there are no other binders for comparison with the same PG grade. Similarly, the results for C 64-28 and A 64-28 are not presented since only two binders of the same grade were tested so no outlier criterion could reasonably be drawn. Figures 3.24-3.27 display the remaining PG grades with multiple binders of the same grade.

A red line is drawn on each graph to emphasize outliers. For PG 58-28 and PG 64-22 (Figures 3.24 and 3.25), any tensile strength below 0.5 MPa was considered an outlier, while for PG 70-22 and PG 76-22 (Figures 3.26 and 3.27) a tensile strength below 0.8 MPa was an outlier. The outlier criteria was arbitrarily chosen by examining the results of each PG grade individually. Figure 3.28 summarizes the results with red indicating outliers, representing the outlier criteria from Figures 3.24-3.27. Source I and F showed a large amount of outliers.

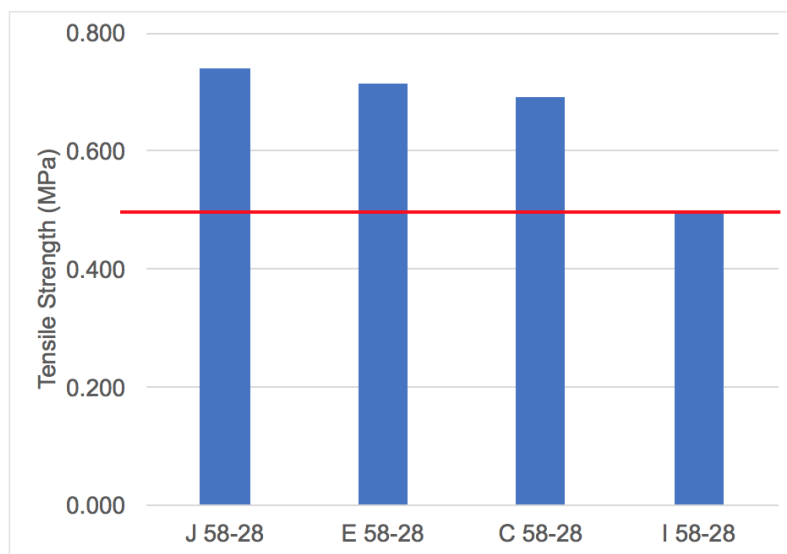


Figure 3.24. The tensile strength at fracture for PG 58-28 binders.

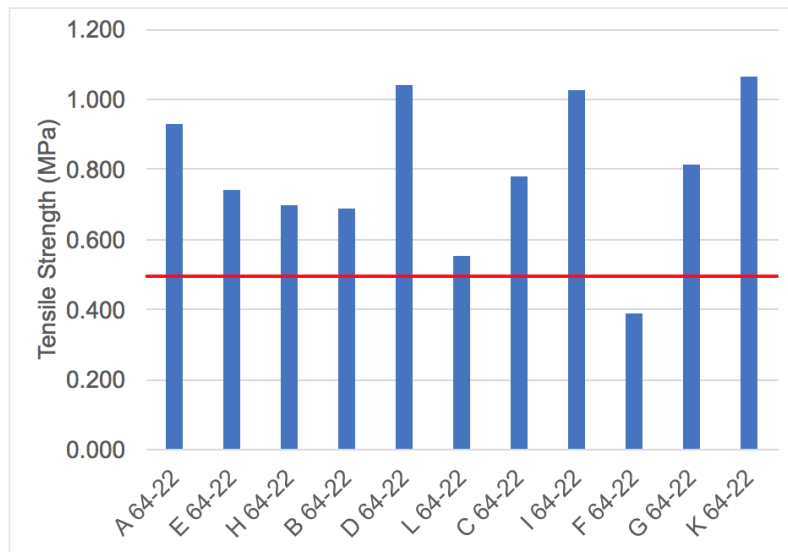


Figure 3.25. The tensile strength at fracture for PG 64-22 binders.

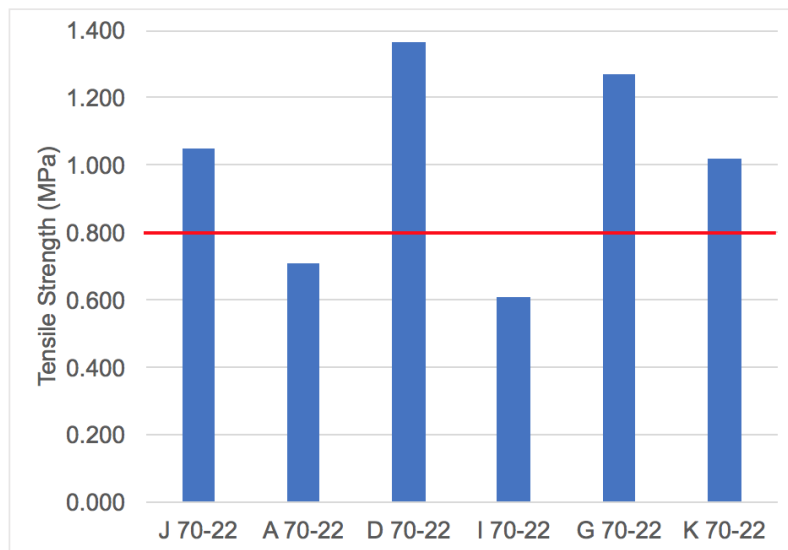


Figure 3.26. The tensile strength at fracture for PG 70-22 binders.

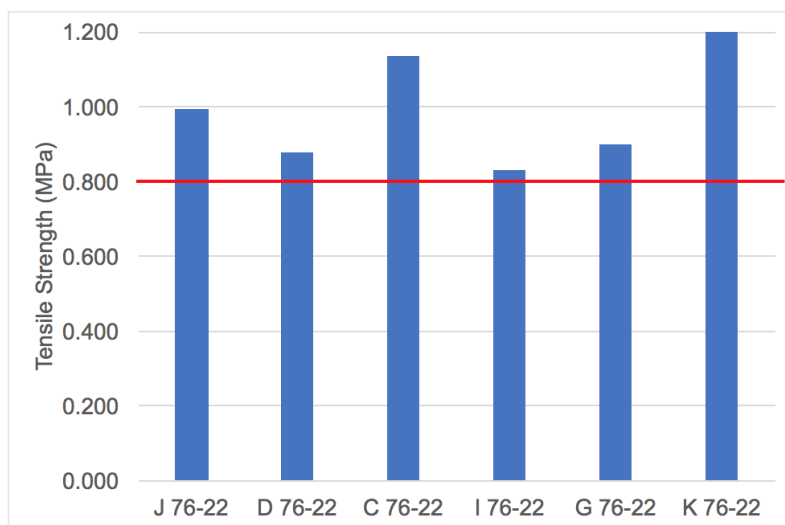


Figure 3.27. The tensile strength at fracture for PG 76-22 binders.

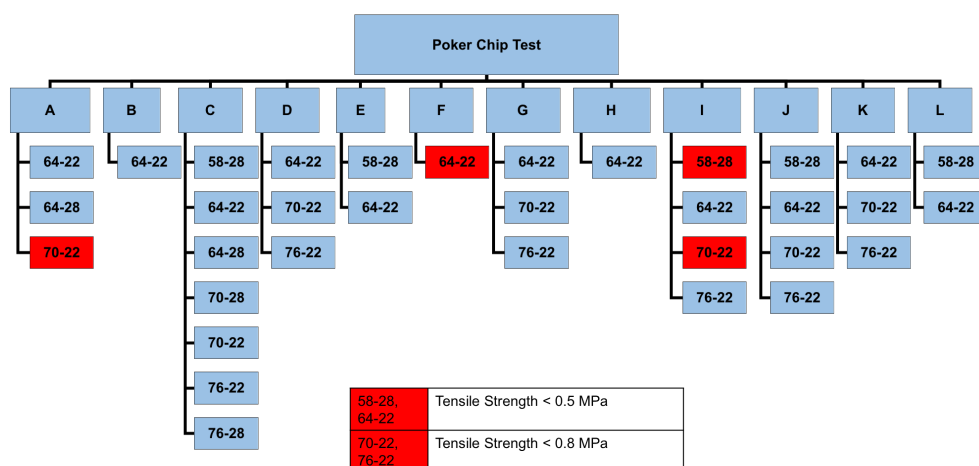


Figure 3.28. A summary of the poker chip test results with outliers in red.

3.2.7 Strength Test at Low Temperature

The BBR Pro was used to test the strength of asphalt binders at two low temperatures for both PAVI and PAVII-aged binders. For the low temperature PG -22 grade, binders were tested at -12°C and -18°C, while PG -28 grade binders were tested at -18°C and -24°C. Similar to the poker chip test in the previous section, the outlier criteria chosen followed no standard and only represents judgment made after compiling the test results.

3.2.7.1 PAVI

Figures 3.29-3.34 show the results of the maximum stress based on the maximum load before fracture for PAVI-aged binders. (Equation 2.6 from the previous chapter was used to calculate the stress). Any binders with a maximum stress less than 1 MPa were considered outliers; the red line on each graph helps point out the outliers. A summary of the results are presented in Figure 3.35. The outliers are in red and brown; the difference in color indicates the outlier at a particular test temperature. For instance, the maximum stress of the low temperature PG -22 binders tested at -12°C and the PG -28 binders tested at -18°C that fall below 1 MPa are in red. A split box indicates that both temperatures tested for that particular binder had a maximum stress below 1 MPa.

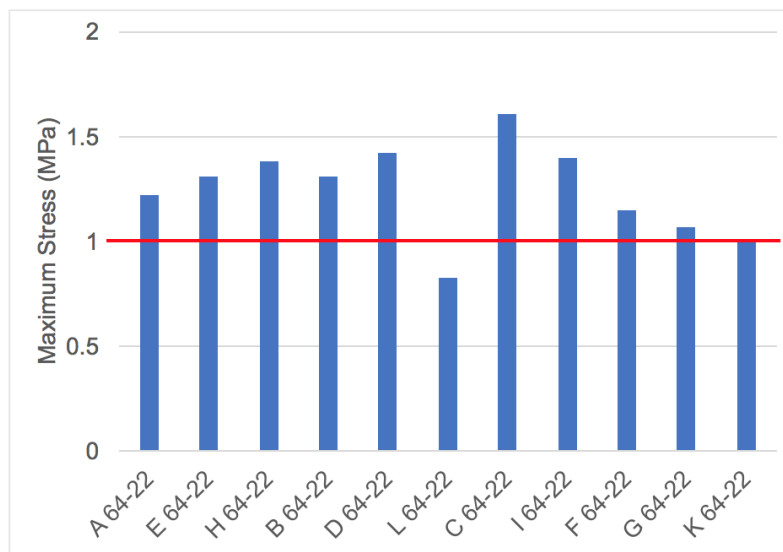


Figure 3.29. The maximum stress at fracture for PG 64-22 PAVI-aged binders tested at -12°C (10°C above the label temperature).

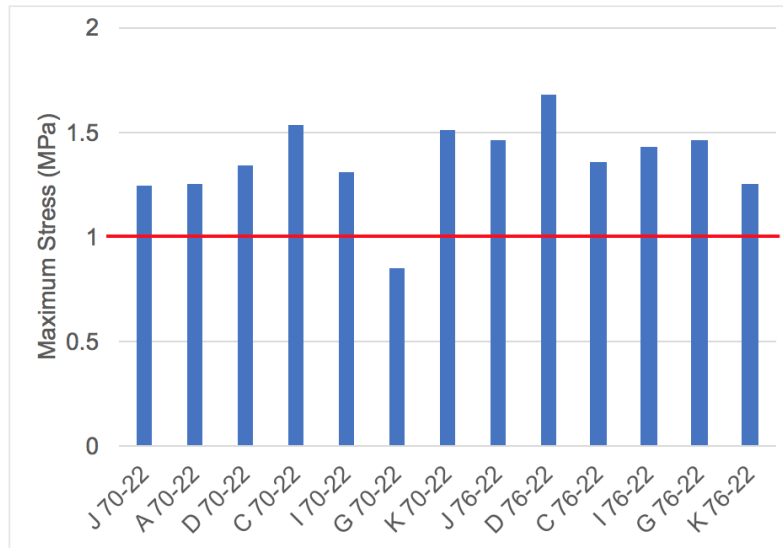


Figure 3.30. The maximum stress at fracture for the remaining low temperature PG -22 PAVI-aged binders tested at -12°C (10°C above the label temperature).

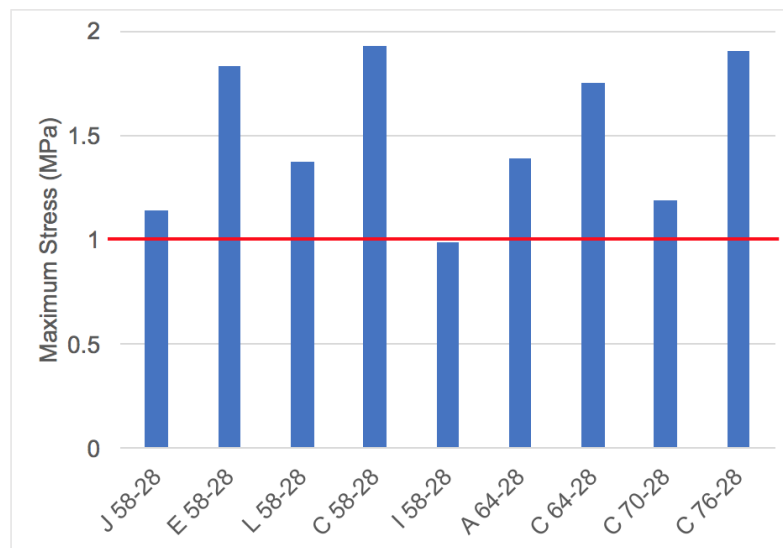


Figure 3.31. The maximum stress at fracture for low temperature PG -28 PAVI-aged binders tested at -18°C (10°C above the label temperature).

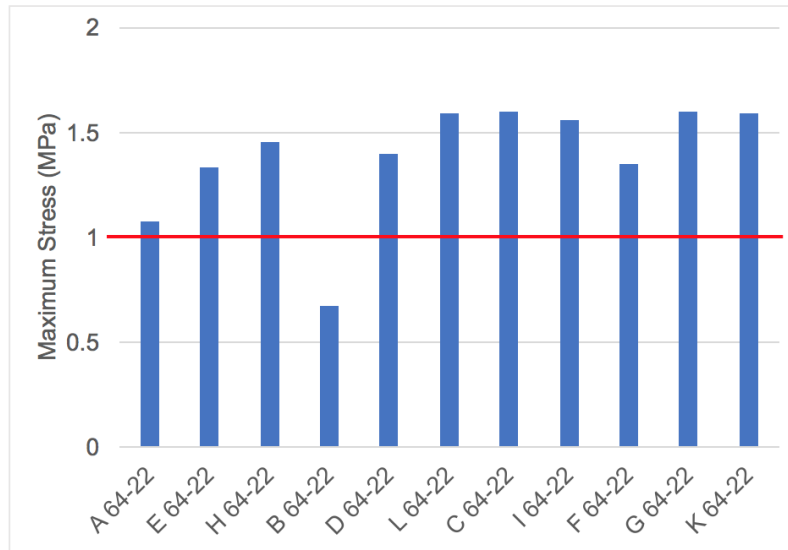


Figure 3.32. The maximum stress at fracture for PG 64-22 PAVI-aged binders tested at -18°C (4°C above the label temperature).

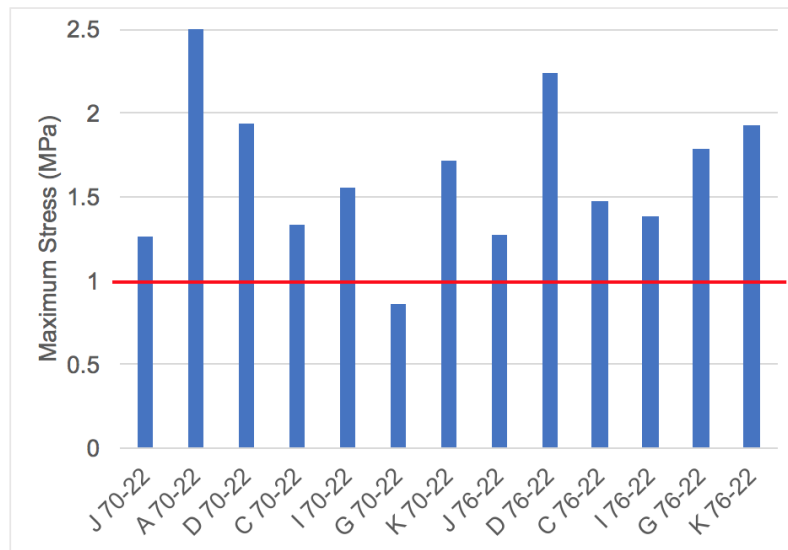


Figure 3.33. The maximum stress at fracture for the remaining low temperature PG -22 PAVI-aged binders tested at -18°C (4°C above the label temperature).

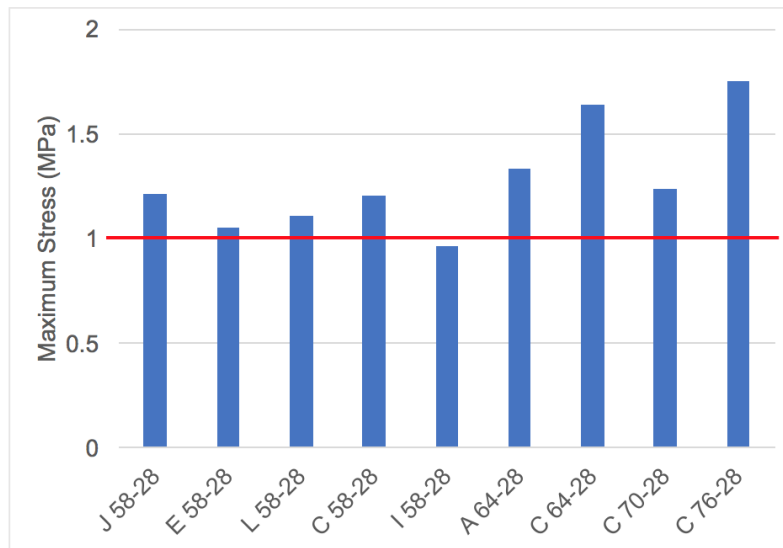


Figure 3.34. The maximum stress at fracture for low temperature PG -28 PAVI-aged binders tested at -24°C (4°C above the label temperature).

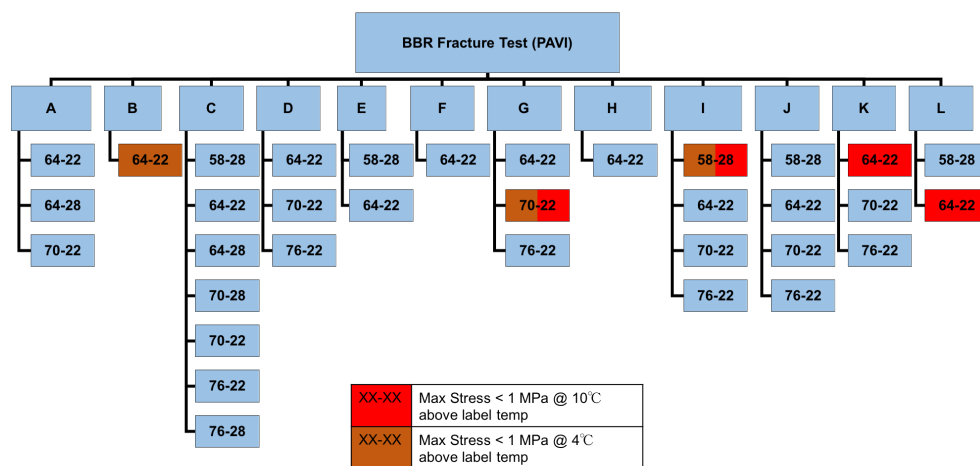


Figure 3.35. Summary of all the strength testing on PAVI-aged binder in the BBR Pro at -12, -18, and -24°C.

3.2.7.2 PAVII

The results of testing done on PAVII-aged binders is shown in Figures 3.36-3.41. Same as the PAVI-aged binders, testing was conducted at 10°C and 4°C above the labeled low temperature PG grade. In addition, the outlier criterion remained at 1 MPa. A summary of the results is displayed in Figure 3.42. Sources C, F, and H showed a high concentration of outliers indicating inadequate strength properties.

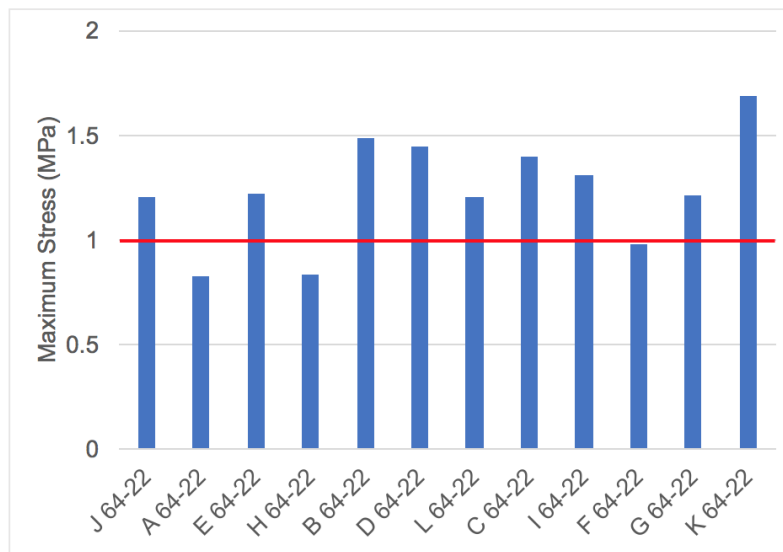


Figure 3.36. The maximum stress at fracture for PG 64-22 PAVII-aged binders tested at -12°C (10°C above the label temperature).

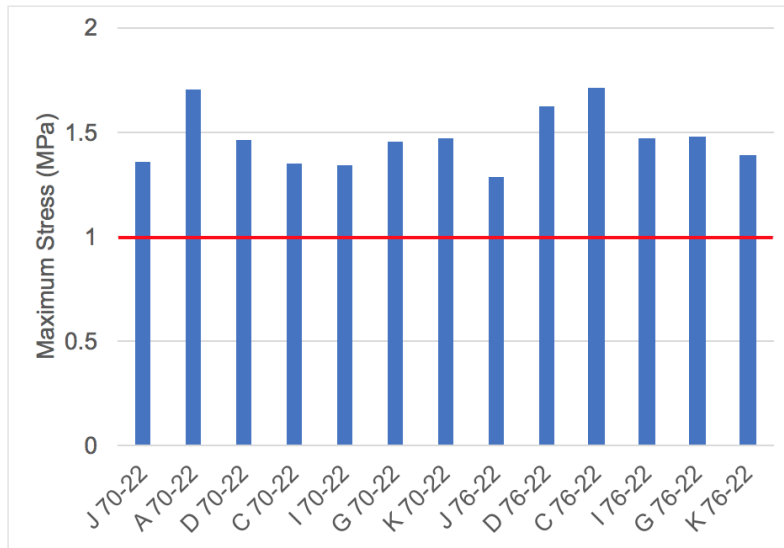


Figure 3.37. The maximum stress at fracture for the remaining low temperature PG -22 PAVII-aged binders tested at -12°C (10°C above the label temperature).

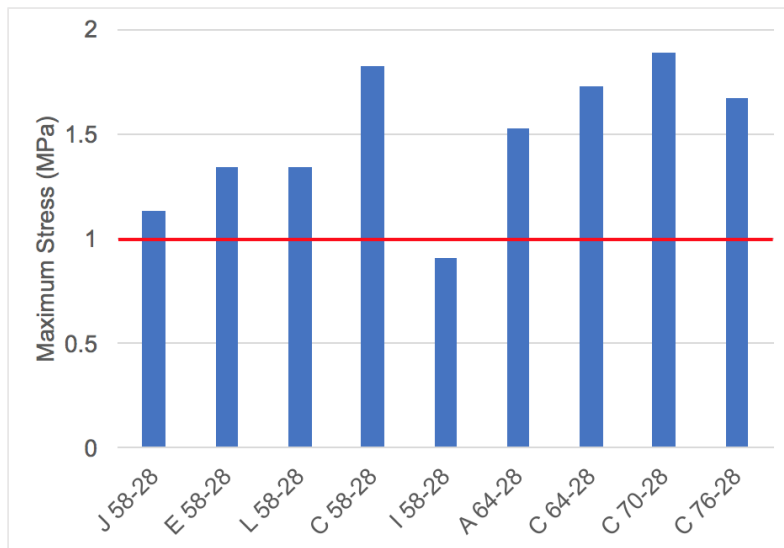


Figure 3.38. The maximum stress at fracture for low temperature PG -28 PAVII-aged binders tested at -18°C (10°C above the label temperature).

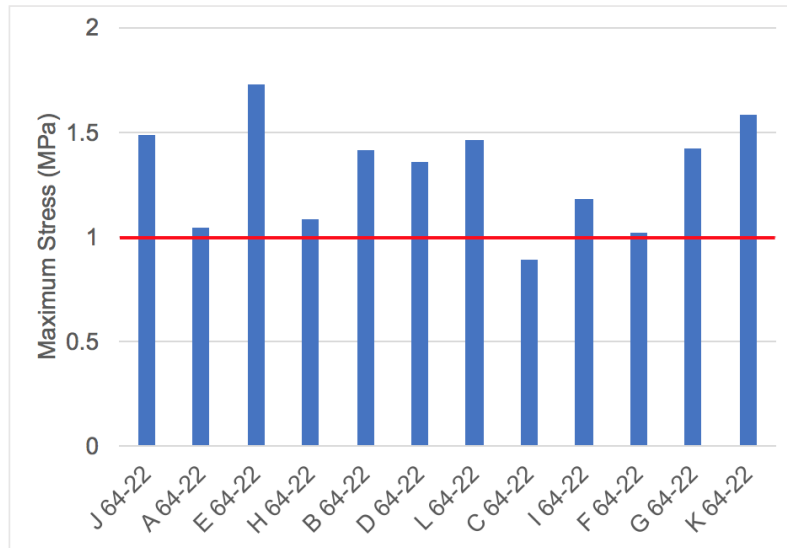


Figure 3.39. The maximum stress at fracture for PG 64-22 PAVII-aged binders tested at -18°C (4°C above the label temperature).

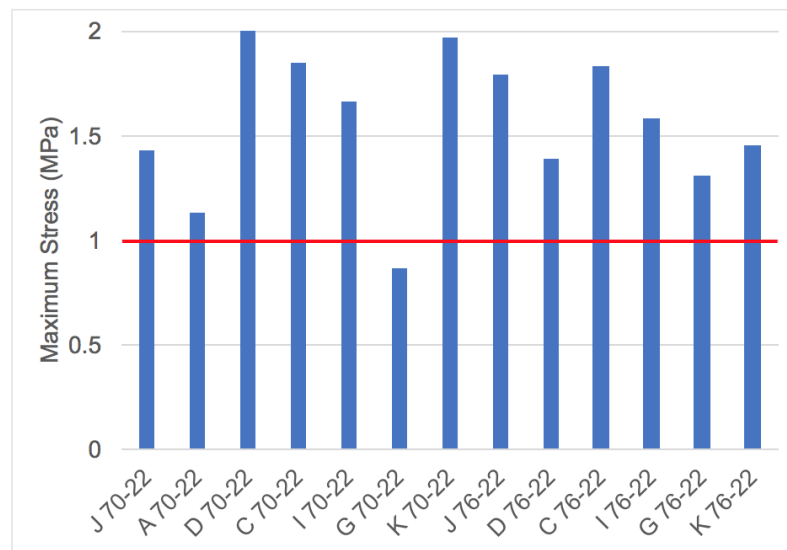


Figure 3.40. The maximum stress at fracture for the remaining low temperature PG -22 PAVII-aged binders tested at -18°C (4°C above the label temperature).

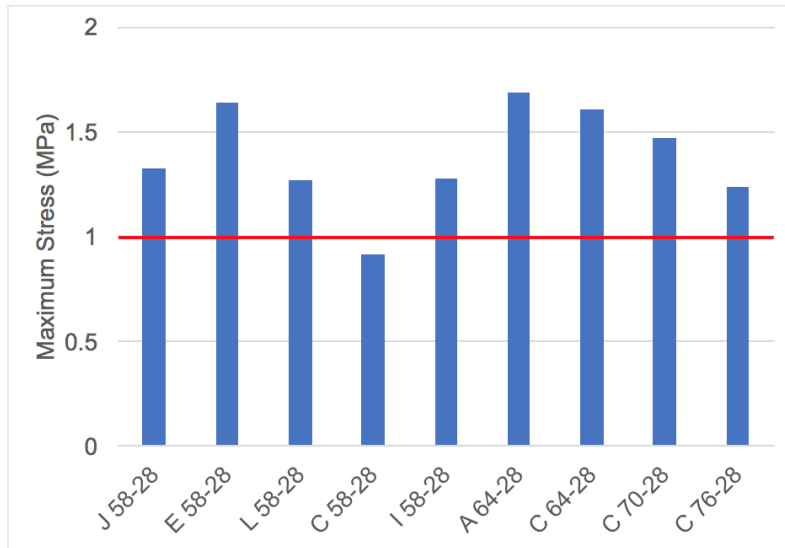


Figure 3.41. The maximum stress at fracture for low temperature PG -28 PAVII-aged binders tested at -24°C (4°C above the label temperature).

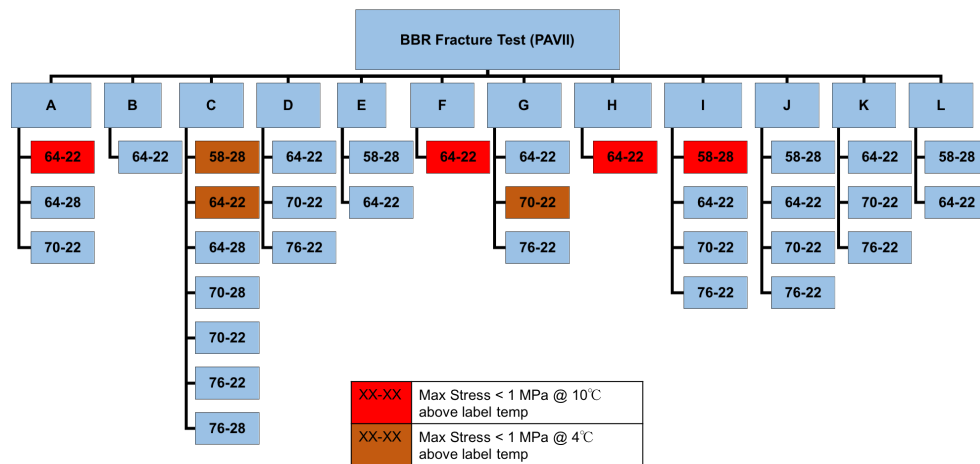


Figure 3.42. Summary of all the strength testing on PAVII-aged binders in the BBR Pro at -12, -18, and -24°C.

CHAPTER 4. CONCLUSIONS AND SUMMARY

4.1 OVERVIEW

Some conclusions can be drawn from the test results gathered during this study. Each test run outside of the PG specification had various outliers, highlighting weaknesses in the PG system. Many binders that passed the PG system testing fell outside of an acceptable range when undergoing other tests not currently part of the PG specification (AASHTO M320). In order to better understand this study's outcomes, Table 4.1 compiles all of the test results to show correlations between asphalt binders.

In Table 4.1, an 'X' represents an outlier, which was defined differently for each test. For the XRF test, any binder that had one or more metals detected (Figure 3.7) was flagged as an outlier. On the other hand, the outliers for the MSCR and spot test, which was a true grade greater than 12°C over the labeled grade for the MSCR test (Figure 3.12) and a black spot area greater than 10% of the total area for the spot test (Figure 3.15), were given an 'X' and the extreme outliers, which was a true grade greater than 90°C for the MSCR test and a black spot area greater than 20% of the total area for the spot test, contributed another 'X'. Thus, the extreme outliers have an 'XX' in its box.

For ΔT_c , outliers were defined as a ΔT_c value greater than 6°C or a stiffness-controlled binder (Figure 3.19), which was translated to an 'X' in Table 4.1. For aging sensitivity and all the strength tests in the BBR Pro, the outliers received an 'X', which was an m-value decrease of greater than 20% or a stiffness increase of greater than 40% for aging sensitivity (Figure 3.23) and a maximum stress less than 1 MPa at 10°C or 4°C above the label temperature for strength tests (Figures 3.35 and 3.42). Those binders that had both outliers present for either aging sensitivity or strength tests were each given an 'XX'. Lastly, the poker chip test was rather straight forward with outliers of a tensile strength less than 0.5 MPa for PG 58-28 and 64-22 and less than a tensile strength of 0.8 MPa for PG 70-22 and 76-22 (Figure 3.28) represented by an 'X'.

The main goal when converting the outliers to 'X's in Table 4.1 was to ensure that each test had fair and equal representation; not one test was given priority over any others. All the 'X's in each row were summed up to find the total number of outliers for each binder; 'XX' was counted as two outliers. Binder I 58-28 had the largest amount of outliers with 7 total, while binder G 70-22 was not far behind with 6 total outliers. In addition, binders A 64-22, C 76-22, F 64-22, I 70-22, J 58-28, and K 76-22 showed a

significant concentration of outliers with 4 total for each binder. It should be noted that these outliers represent neither a negative nor positive property. Not enough information is known as to whether the mixtures with these outlier binders perform better or worse than the average mixture.

These results show that while the PG system is a step forward from grading systems of the past, such as penetration and viscosity, many improvements still need to be made to better characterize asphalt binders in order to best predict field performance. These binders had chemical or mechanical characteristics that were different from other similarly graded binders. These differences are not captured by tests included in the current PG specification (AASHTO M320). Thus moving forward, binders from various sources and PG grades need to undergo testing within and outside of the PG system to develop a better understanding of the true performance characteristics of asphalt binders.

The additional testing conducted in this study does not provide sufficient information to better grade binders compared to the current PG system in place. More data on binders with varying chemical compositions will make the asphalt binder screening process more robust, providing links to make valuable correlations. This study cataloged 34 binders relevant to Texas climate and sources, but more work needs to be done to grow this catalog within Texas and nationwide. Finally, it is noted that the outliers identified in this study were based on deviation from binders with similar PG grades. Linking asphalt binder and mixture testing is crucial to determine if the outliers discovered in this study are favorable or destructive asphalt properties. Further performance testing, preferably on mixtures, is required to establish whether such behavior is beneficial (i.e. PG does not recognize better performing binders) or detrimental (i.e. PG does not identify damage susceptible binders) to mixture and pavement performance.

Table 4.1. A summary of the outliers for all the tests run in this study.

	Tests								
Binder Name	XRF	MSCR	Spot	Delta Tc	Aging Sensitivity	Poker Chip	BBR Fracture (PAVI)	BBR Fracture (PAVII)	Total
A 64-22	X				XX			X	4
A 64-28	X								1
A 70-22	X					X			2
B 64-22							X		1
C 58-28								X	1
C 64-22								X	1
C 64-28									0
C 70-28		X	X						2
C 70-22		XX	X						3
C 76-22		X	XX		X				4
C 76-28		X							1
D 64-22									0
D 70-22									0
D 76-22									0
E 58-28				X	XX				3
E 64-22									0
F 64-22	X			X		X		X	4
G 64-22				X					1
G 70-22	X		X	X			XX	X	6
G 76-22		XX		X					3
H 64-22				X				X	2
I 58-28			XX	X		X	XX	X	7
I 64-22									0
I 70-22	X	X	X			X			4
I 76-22	X								1
J 58-28	X		XX	X					4
J 64-22		X							1
J 70-22				X					1
J 76-22	X			X					2
K 64-22							X		1
K 70-22					X				1
K 76-22			XX	X	X				4
L 58-28	X			X	X				3
L 64-22	X						X		2

REFERENCES

- Anderson, M. R., King, G. N., Hanson, D. I., and Blankenship, P. B. (2011). Evaluation of the Relationship between Asphalt Binder Properties and Non-Load Related Cracking. *Asphalt Paving Technology*, 80:615–663.
- Arega, Z., Sakib, N., Bhasin, A., and Peterson, J. (2016). An Investigation into the Continuous High-Temperature Grade and Elastic Recovery of Asphalt Binders Measured using the Creep-Recovery Test. *Journal of Testing and Evaluation*.
- Arnold, T. and Shastry, A. (2015). Analysis of Asphalt Binders for Recycled Engine Oil Bottoms by X-ray Fluorescence Spectroscopy. *TRB 94th Annual Meeting Compendium of Papers*.
- ASTM 7643 (2010). Standard Practice for Determining the Continuous Grading Temperatures and Continuous Grades for PG Graded Asphalt Binders. *Annual Book of American Society for Testing Materials: ASTM Standards*.
- Bahia, H. U., Hanson, D. I., Zeng, M., Zhai, H., Khatri, M. A., and Anderson, R. M. (2001). NCHRP Report 459: Characterization of Modified Asphalt Binders in Superpave Mix Design. Technical report, Nation Cooperative Highway Research Program, Washington, DC.
- Bahia, H. U., Zhai, H., Bonnetti, K., and Kose, S. (1999). Non-Linear Viscoelastic and Fatigue Properties of Asphalt Binders. In *Association of Asphalt Paving Technologists*, Chicago.
- Blow, M. D. (2016). Asphalt Binder Basics, Specifications, History and Future. In *North Dakota Asphalt Conference*. Asphalt Institute.
- Brown, E. R., Kandhal, P. S., Roberts, F. L., Kim, Y. R., Lee, D.-Y., and Kennedy, T. W. (2009). *Hot Mix Asphalt Materials, Mixture Design and Construction: Third Edition*. NAPA Research and Education Foundation, Lanham.
- Bukowski, J., Youtcheff, J., and Harman, T. (2011). The Multiple Stress Creep Recovery (MSCR) Procedure. *Federal Highway Administration's (FHWA's) Asphalt Pavement Technology Program*.

- D'Angelo, J. (2010). New High-Temperature Binder Specification Using Multistress Creep and Recovery. *Transportation Research Board*, E-C147(December):1–34.
- Dubois, E., Mehta, D. Y., and Nolan, A. (2014). Correlation between Multiple Stress Creep Recovery (MSCR) Results and Polymer Modification of Binder. *Construction and Building Materials*, 65:184–190.
- Falchetto, A. C., Marasteanu, M. O., Balmurugan, S., and Negulescu, I. I. (2014). Investigation of Asphalt Mixture Strength at Low Temperatures with the Bending Beam Rheometer. *Road Materials and Pavement Design*, 15(S1):28–44.
- Glover, C. J., Davison, R. R., Domke, C. H., Ruan, Y., Juristyarini, P., Knorr, D. B., and Jung, S. H. (2005). Development of a New Method for Assessing Asphalt Binder Durability with Field Validation. Technical report, Texas Transportation Institute.
- Hajj, R. (2016). *Fatigue Characterization of Asphalt Binders Using a Thin Film Poker Chip Test*. Master's thesis, The University of Texas at Austin.
- Hajj, R. and Bhasin, A. (2017). The Search for a Measure of Fatigue Cracking in Asphalt Binders - A Review of Different Approaches. *International Journal of Pavement Engineering*, 8436(February).
- Jones, Z., Romero, P., and VanFrank, K. (2014). Development of Low-Temperature Performance Specifications for Asphalt Mixtures using the Bending Beam Rheometer. *Road Materials and Pavement Design*, 15(3):574–587.
- Kennedy, T. W., Huber, G. A., Harrigan, E. T., Cominsky, R. J., Hughes, C. S., Quintus, H. V., and Moulthrop, J. S. (1994). Superior Performing Asphalt Pavements: The Product of the SHRP Asphalt Research Program. Technical report, Strategic Highway Research Program, Washington, DC.
- Marasteanu, M. (2004). Role of Bending Beam Rheometer Parameters in Thermal Stress Calculations. *Transportation Research Record*.
- Masad, E., Somadevan, N., Bahia, H. U., and Kose, S. (2001). Modeling and Experimental Measurements of Strain Distribution in Asphalt Mixes. *Journal of Transportation Engineering*, 127(December):477–485.

- Root, R. E. and Moore, R. B. (1992). The Use of Conversion Residue as a Component in Asphalt Cement. Technical report, Strategic Highway Research Program, Washington, DC.
- Rowe, G. (2016). Delta Tc-Some Thoughts on the Historical Development. In *Binder ETG Meeting*.
- Stuart, K. and Mogawer, D. (2002). Validation of the Superpave Asphalt Binder Fatigue Cracking Parameter using the FHWA's Accelerated Loading Facility. *Asphalt Paving Technology*.
- Sultana, S. (2014). *Tensile Strength of Asphalt Binder and Influence of Chemical Composition on Binder Rheology and Strength*. Ph.d. dissertation, The University of Texas at Austin.
- Texas Department of Transportation (2006). Superpave Binder Specification.
- Texas Department of Transportation (2014). Standard Specifications for Construction and Maintenance of Highways, Streets, and Bridges.
- Tsai, B. and Monismith, C. (2005). Influence of Asphalt Binder Properties on the Fatigue Performance of Asphalt Concrete Pavements. *Journal of the Association of Asphalt Paving Technologists*, 74(January):733–789.
- Zhou, F., Li, H., Chen, P., and Scullion, T. (2014). Laboratory Evaluation of Asphalt Binder Rutting, Fracture, and Adhesion Tests. Technical report, Texas A&M Transportation Institute, College Station.